

Full Length Research Paper

Future evolution of surface temperature extremes and the potential impacts on the human health in Senegal

Sarr A. B., Diba I., Basse J., Sabaly H. N. and Camara M.*

Laboratoire d'Océanographie, des Sciences de l'Environnement et du Climat (LOSEC),
UFR Sciences et Technologies, Université Assane SECK de Ziguinchor, Sénégal.

Received 19 September, 2019; Accepted 4 November, 2019

Climate change impacts negatively vulnerable regions such as West African countries like Senegal, through an increase of climate extremes. The objectives of this study is to analyze the future evolution of the extreme temperature events and their impacts on human health in Senegal during the cold (DJF), hot (MAM) and wet seasons (JAS) under the greenhouse gas scenarios RCP4.5 and RCP8.5 using Climate projections of five (5) regional climate models (RCMs) of the Coordinated Regional Climate Downscaling Experiment (CORDEX) program. The results show that the biases of the RCMs are globally low especially their ensemble mean of the RCMs. This ensemble mean was afterwards considered in the analysis of the climate extremes in the near (2021-2050) and far future (2071-2100). When considering the near future, the frequency of the hot nights (Tn90p) increases under the scenario RCP8.5 (up to 90%) during the rainy season in the south of the country. As for the percentage of the hot days (Tx90p), it may reach approximately 70% under the scenario RCP8.5 in DJF over the majority of the country. Moreover, a strong increase of Tn90p and Tx90p is also diagnosed during the far future with values exceeding 80% over most parts of the country. Concerning the evolution of the heat wave magnitude index-daily, the ensemble mean of all models shows that the heat waves are more severe in MAM and JAS under both scenarios during the near and the far future over most parts of the country. To estimate the potential impacts of this heat stress on the human health, the heat index and the humidex are used. The analysis of the heat index shows that the sanitary risks are more perceptible over the whole country during the rainy season with values reaching the symptom band II for both scenarios during the far future. As for the humidex, it is characterized by a gradual increase from the historical period to the far future. This analysis highlights the fact that appropriate adaptation measures should be considered to tackle efficiently the increase of temperature extremes which may impact negatively the human health.

Key words: Regional climate models, CORDEX, climate indices, heat stress, climate scenarios, Senegal.

INTRODUCTION

The knowledge of extreme events of temperatures is of a key importance for several economic sectors,

*Corresponding author. E-mail: moctar.camara@univ-zig.sn or moctar1sn@yahoo.fr.

particularly for agriculture. Indeed, these extreme events can impact strongly the West African populations. Agriculture, which is the main source of income for the populations of this region, and particularly those of Senegal, is the most sensitive sector to these extreme changes in temperature. Indeed, very large increases in temperature can inhibit the growth of certain plants (Salack et al., 2015; Basak et al., 2013). Thus, yields of some crops such as wheat, rice, maize or groundnuts can be greatly reduced by extremely high temperatures at the key stage of their development. These temperature increases can also have negative impacts on human health as some studies have shown (Campbell et al., 2018; Hass et al., 2016; Garland et al., 2015). According to Kotir (2011), the African continent is generally considered as warm and dry continent with current trends showing warmer heat waves than those that prevailed 100 years ago. The mean temperatures observed show an increase in global warming since 1960 (IPCC, 2013).

Recent studies led by Moron et al. (2016), Ly et al. (2013) and New et al. (2006) showed an increase in heat waves and a decrease in cold days over West Africa. In addition, the minimum temperature increases more rapidly than the maximum temperature, thus involving a reduction of the diurnal variation in temperature. The predictions of models based on greenhouse gas emissions scenarios showed that the global warming continues to increase (Ceccherini et al., 2017; Sylla et al., 2016; Giorgi et al., 2014; Boko et al., 2007). However, these temperature changes are not uniform. Indeed, the climate change scenarios used in West Africa showed that the greatest temperature rises are recorded in semi-arid areas such as the Sahara and the Sahel and the lowest in the lower latitudes, especially in the Guinean zone (Hulme et al., 2001). At the beginning, these climate change scenarios were done with global climate models (IPCC, 2013). However, these global climate models (GCMs) face enormous difficulties in representing the climate at the regional scale because of their low spatial resolution (200 to 300 km). Certainly, these GCMs do not take into account certain surface processes such as topography or heterogeneities of the Earth's surface. To remedy it, regional climate models (RCMs) are increasingly being used to dynamically disaggregate GCMs (Giorgi et al., 2014; Laprise et al., 2013; Camara et al., 2013).

In this paper, we analyze the future evolution of temperature extremes and perceived heat indices (humidex and heat index) in Senegal using regional climate models of the Coordinated Regional Climate Downscaling EXperiment (CORDEX programme) during the future under the scenarios RCP4.5 and RCP8.5. This program is described in detail by Giorgi et al. (2009). The CORDEX is an international program led by a number of research centers to provide the scientific community with reliable climate change scenarios for

impact assessment and research adaptation. Two types of simulations are considered: those concerning the present time and the climate projections. The first category of simulations (present time) consists of evaluating the performance of RCMs to reproduce the present climate (1989-2008). Studies led in this context (Gbobaniyi et al., 2014; Kim et al., 2014; Nikulin et al., 2012; Camara et al., 2013) have shown that these CORDEX RCMs represent well enough the spatial distribution of rainfall and temperature and also the ensemble mean of the models outperforms the regional climate models taken individually.

The second series of simulations (climate projections, period 2006-2100) aims to analyze the future evolution of the climate. In this context, several studies have been carried out (Sarr and Camara, 2017; Diallo et al., 2016; Sylla et al., 2016; Mariotti et al., 2014; Giorgi et al., 2014; Laprise et al., 2013) to identify the future evolution of the precipitation and the mean surface temperature. However, few research works have been devoted in studying the future evolution of extreme temperature events and its impact on human health in West Africa and particularly in Senegal. Then, the main purpose of this study is to analyze the seasonal evolution of temperature extremes and their impacts on human health in Senegal by focusing on greenhouse gas concentration scenarios RCP85 and RCP4.5.

DATA AND METHODS

Description of the study area

Senegal is an African country located in the westernmost part of the continent (Figure 1). It extends in longitude between 12° W and 17° W and in latitude between 12° N and 16.5°N in the so-called Sudano-Sahelian region. This latter is considered by the Intergovernmental Panel on Climate Change (IPCC) experts as an area vulnerable to climate change due to its low capacity adaptation (Boko et al., 2007; IPCC, 2013). The climate in Senegal is characterized by a single rainy season (roughly from June to October) followed by a longer dry season (November to May). During the rainy season, rainfall decreases from South to North; this translates into a semi-arid type climate in the North and a tropical one in the South (Sagna, 2000).

Climate change scenarios and climate indices

A study based on daily temperature data is done using high resolution simulations (0.44°) of five (5) regional climate models (RCMs) of the CORDEX program. These models are: CCLM4, RCA4, HIRHAM5, RACMO22T and REMO. The institutions of these models and their references are presented in Table 1. The RCMs outputs are available from this website: <https://www.cordex.org/output.html>. These models are described in details by Nikulin et al. (2012). The RCMs RACMO22T, HIRHAM5 and REMO are forced by the outputs of the GCM EC-EARTH; while models RCA4 and CCLM4 are forced by the outputs of the GCM CNRM-CM5. The climate projections were obtained by forcing these RCMs through the outputs of these GCMs under the greenhouse gas scenarios RCP4.5 (medium scenario) and RCP8.5



Figure 1. Map of Africa. The study area (Senegal) is in red color.

Table 1. Description of the regional climate models.

| Name | GCM forcing | Institution | References |
|----------|-------------|-----------------------|-----------------------------|
| CCLM4 | CNRM-CM5 | CLM-community | Baldauf et al. (2011) |
| RACMO22T | EC-EARTH | KNMI, The Netherlands | Van Meijgaard et al. (2008) |
| RCA4 | CNRM-CM5 | SMHI, Sweden | Samuelsson et al. (2011) |
| HIRHAM5 | EC-EARTH | DMI, Denmark | Christensen et al. (2006) |
| REMO | EC-EARTH | MPI, Germany | Jacob et al. (2007) |

Table 2. Description of the climate indices

| Indices | Descriptive name | Definition | Unit |
|---------|--------------------------|---|------|
| Tn90p | Frequency of warm nights | Percentage of nights with daily minimum temperatures $T_n > 90$ th percentile of the reference period (1976-2005) | % |
| Tx90p | Frequency of warm days | Percentage of days with daily maximum temperatures $T_x > 90$ th percentile of the reference period (1976-2005) | % |

(severe scenario), corresponding respectively to an emission of 4.5 and 8.5 W/m^2 by 2100 (Moss et al., 2010). To study the future evolution of temperature extremes in Senegal, we considered the periods 1976-2005 (reference period), 2021-2050

(near future) and 2071-2100 (far future). Some climate indices relevant for the characterization of the temperature extremes are analyzed (Table 2).

In addition to these indices presented in Table 2, we also used

the heat waves magnitude index- daily (HWMId) (Russo et al., 2015). The HWMId is defined as the maximum of all heat wave magnitudes for a given year, where heat wave is the period of 3 or more consecutive days with maximum temperature above the daily threshold for the reference period 1976-2005. The threshold is defined as the 90th percentile of daily maxima, centered on a 31-day window. This index is designed to take into account both the severity of temperature extremes and the duration of a heat wave. The magnitude of a heatwave is defined as the sum of the daily magnitude (Md) within a heatwave. Md is given by:

$$M_d = \begin{cases} \frac{T_d - T_{75p}}{T_{75p} - T_{25p}}, T_d > T_{25p} \\ 0, T_d \leq T_{25p} \end{cases} \quad (1)$$

where T_d is the daily maximum temperature, T_{75p} and T_{25p} are respectively the 75 and 25th percentile values of the yearly maximum temperature during the reference period (1976-2005).

To assess the heat stress, we considered the two main standard heat indices used in numerous studies (Garland et al., 2015; Anderson et al., 2013; Willett and Sherwood, 2012; Hayhoe et al., 2010): the heat index (HI) developed by the US National Weather Service and the humidity-index commonly called humidex (HUM) developed by the Canadian meteorologists. The HI measures the combined effect of heat and humidity on human physiology while the HUM was used to describe the impacts of humidity on human comfort.

The heat index (HI) and the humidex (HUM) are respectively defined by the Equations 2 and 3:

$$HI = -42.379 + 2.04901523T + 10.143333129R - 0.224755417R - 6.83783 \times 10^{-3}T^2 - 5.481717 \times 10^{-2}R^2 + 1.22874 \times 10^{-3}T^2R + 8.5282 \times 10^{-4}TR^2 - 1.99 \times 10^{-6}T^2R^2 \quad (2)$$

where HI is the heat index (in °F), T is the 2 m air temperature (in °F) and R is the 2 m relative humidity (in %). In this study, the HI values were afterwards converted into °C.

$$HUM = T + 59(e - 10) \quad (3)$$

where $e = 6.112 \times 10^{7.5T / (237.7 + T)} \cdot R / 100$. T and HUM are respectively the 2 m air temperature (°C) and the humidex (°C)

The analysis of these climate indices is carried out during the hot (March-April-May, MAM), cold (December-January-February, DJF) as well as the rainy (July-August-September, JAS) seasons.

RESULTS

Validation of the surface temperature

Figure 2 shows the evolution of the mean surface temperature during DJF (average from December to February), MAM (average from March to May) and JAS (average from July to September) periods from 1989 to 2008 for the Climate Research Unit (CRU) observation data and the deviation from CRU of the ensemble mean of the models. The CRU data shows that the lowest temperatures (around 24°C) are observed during the DJF period and especially in the northwestern part of Senegal. During the MAM period, temperatures are relatively high through Senegal compared to other

seasons. In addition, CRU climatology has a zonal gradient with higher temperatures observed towards the east of the country during this period. However, during the rainy season (JAS), it has a decreasing north-south gradient over Senegal. This is due to the fact that during this season, the rainfall in this country is characterized by a latitudinal gradient with intensities much stronger in the south causing a considerable temperature declines in this part of the country. When considering the deviation from CRU of the ensemble mean of the models, weak warm biases (less than 1.5°C) are recorded in DJF over the country especially in the southern and north-eastern parts over the western part of the country and weak cold bias over the coastal zone. The deviation from CRU of the ensemble mean during the summer period (JAS) shows that the ensemble mean of all models reproduces well the spatial pattern of the temperature over the country with an underestimation over the southern part where it has a very low underestimation (less than 1°C). When comparing the performance of individual models with the ensemble of all models (Figure not shown), we found that biases are weaker for the latter; in coherence with Gbobaniyi et al. (2014) and Kim et al. (2014) works which showed that the ensemble mean of the models better reproduces the spatial distribution of surface temperature (Appendix Figures 1-4). These small biases also confirm that the ensemble mean of all models has a more robust signal.

This validation study allowed us to confirm that the ensemble mean of the models improves the performance of the models taken individually as shown in the previous studies (Gbobaniyi et al., 2014; Kim et al., 2014). That is why it will be considered to diagnose the future evolution of temperature and some extreme temperature indices in Senegal.

Future evolution of the mean surface temperature

The spatial distribution of the mean surface temperature difference between the near future (2021-2050) and the reference period (1976-2005) shows that the ensemble mean of the models shows an increase of the mean temperature during all three considered seasons (Appendix Figures 5). These increases are generally higher during the cold season (DJF) and can exceed 1.5°C, over large parts of the country under the severe scenario (RCP8.5). The east-west gradient during the MAM season is materialized by increases which are stronger towards the eastern part of the country. This warming could exceed 1°C under the medium scenario and 1.3°C under the severe one. Temperature increases are relatively lower during the rainy season (JAS) compared to the other seasons. The largest increases are in the northeastern part of the country and do not exceed 1.2°C under the severe scenario. Senegal could experience a very strong rise in temperatures during the far future compared to the near future. The highest

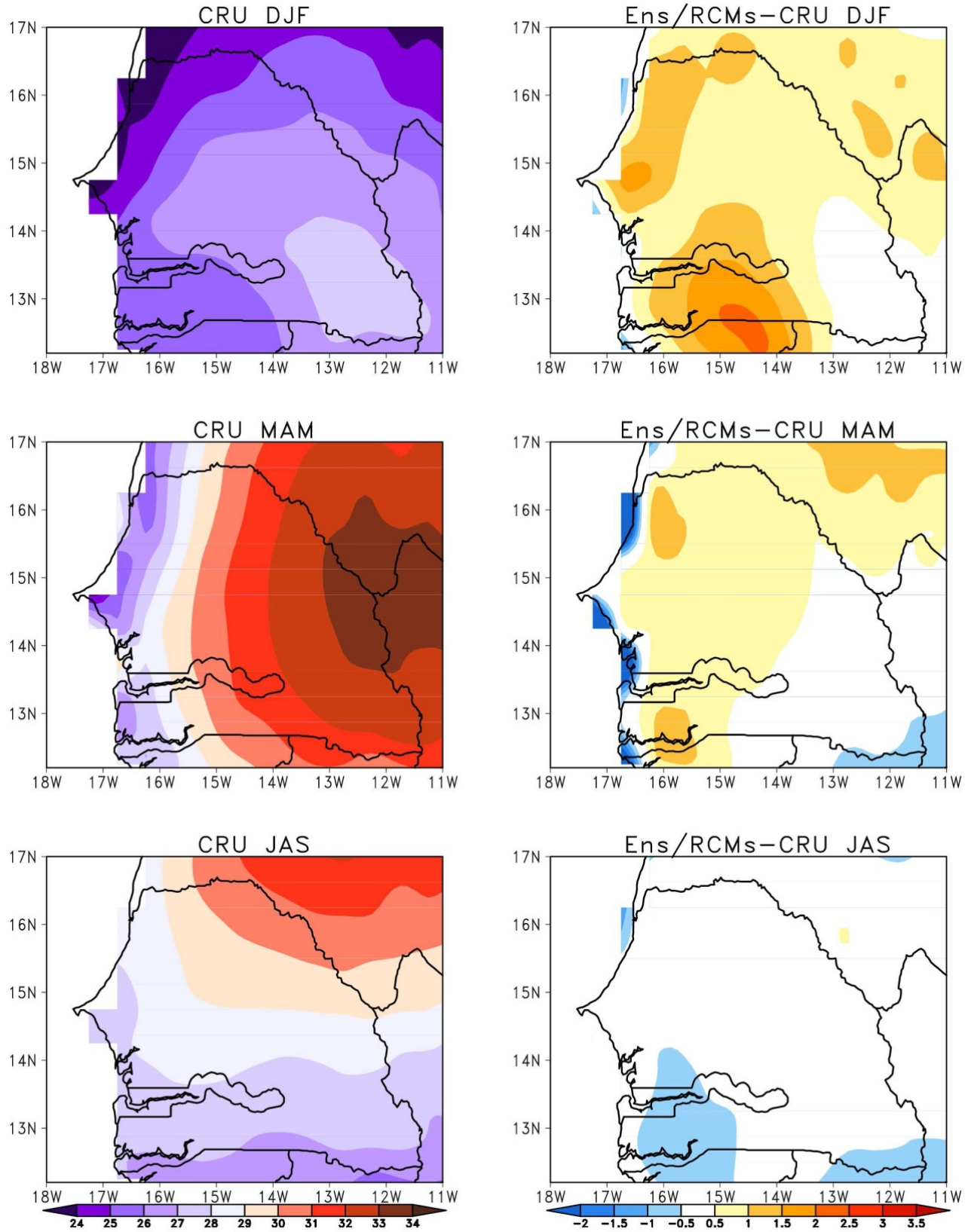


Figure 2. Mean temperature in DJF, MAM and JAS seasons from 1989 to 2008 for CRU data and deviation from CRU observations of mean DJF, MAM and JAS temperature averaged from 1989 to 2008 of the ensemble mean of regional climate models (RCMs).

increases are still observed in DJF in the center of the country and can exceed 2°C under the medium scenario and 4.4°C under the severe one. These temperature increases are relatively low in the north and the south of the country. In MAM, the ensemble mean of the models under the RCP4.5 and RCP8.5 scenarios simulates temperature increases of up to 2 and 4.2°C, respectively in the eastern part of the country. As for the near future, the highest temperature increases in JAS are still recorded in the north-east and can exceed 2.3 and 4°C, respectively under the scenarios RCP4.5 and RCP8.5 during the far future. These strong temperature increases observed in the semi-arid countries of Sahel and particularly in Senegal may lead to an increase in evaporation phenomena and consequently a strengthening of rainfall extreme events such as floods as pointed by Ly et al. (2013).

Future evolution of temperature extremes

Figure 3 shows the frequency of days during the near future with minimum temperature warmer than the 90th percentile of the reference period (1976-2005) threshold for the three seasons considered (DJF, MAM, JAS). The ensemble mean of the models under both scenarios shows a strong percentage of warm night (Tn90p) in DJF over the center of the country with values exceeding 70%. During the MAM and JAS seasons, the ensemble mean of the models presents a north-south gradient with values exceeding 90% during the JAS season over the south of the country for both scenarios. The Tn90p spatial evolution during the far future (2071-2100) (Figure 4) shows that the ensemble mean of the models predicts a stronger change during the far future compared to the near future. In fact, during the cold season (DJF), it projects Tn90p values of the order of 80% under the medium scenario (RCP4.5). Under the severe scenario (RCP8.5), it envisages very strong changes especially over the coastal zone (greater than 98%). In MAM, large increase in the percentage of warm nights during the far future are recorded in the south of the country and can exceed 99% under the RCP8.5 scenario. This increase in warm nights is consistent with the larger surface temperature in the MAM season known as the hottest one. Moreover, the greenhouse gas concentration in the atmosphere tends to increase during the far future under the severe scenario RCP8.5 which in turn may increase surface temperature and thermal extremes. The frequency of warm nights is generally higher during the JAS season through Senegal, especially under the RCP8.5 scenario with values close to 100% by 2100. The larger increase in the percentage of warm nights (Tn90p) is consistent with the faster strengthening of minimum temperatures compared to maximum temperatures in the Sudano-Sahelian region

as suggested by New et al. (2006), Ly et al. (2013) and CEDEAO-ClubSahel/OCDE/CILSS (2008).

The percentage of days with maximum temperature greater than the 90th percentile (Tx90p) of the reference period during the near future is shown in Figure 5. The ensemble mean of the models, under both scenarios, projects a frequency of Tx90p of the order of 70% over a large part of the country in DJF. During the hot season (MAM), it projects small changes in hot days (Tx90p). The highest values of Tx90p recorded in the country are of the order of 60% for the severe scenario (RCP8.5). The changes are generally lower in the coastal zone for both scenarios. This result suggests some possible sea effects as this latter may decrease the surface temperature which in turn may impact temperature extremes. Tx90p changes by 2050 are generally low in JAS compared to the cold season (DJF) and hot season (MAM). Indeed, the highest values are obtained with the RCP8.5 scenario (less than 60%) over a large part of the country. Stronger values of Tx90p are recorded when considering the far future (Figure 6). In DJF, the ensemble mean of the models presents a north-south gradient of Tx90p with a hot day frequency reaching 94% under the RCP4.5 scenario and 98.5% under the RCP8.5 scenario in the south of the country. On the other hand, during the hot season (MAM), the ensemble mean of the models has an east-west gradient with an important increase in the occurrence of hot days (up to 97%) towards the west during this period under the severe scenario (RCP8.5). Projected changes during the far future of Tx90p in JAS under the medium scenario are relatively low with values not exceeding 70% over a large part of the country. However, under the severe scenario, it predicts very strong changes (above 93%) over Senegal. This could translate into negative consequences for the socio-economic activities such as agriculture and the human health. Projected changes during the far future of Tx90p in JAS under the medium scenario are relatively low with values not exceeding 70% over a large part of the country. But, under the severe scenario, it predicts very strong changes (above 93%) over the country.

To go deeper in the analysis of thermal extremes, Figure 7 shows the heat waves magnitude index-daily (HWMId) during the near future (2021-2050). In DJF, the ensemble mean of the models under both scenarios presents heat waves with magnitude of the order of 35 over a large part of the country. Values reaching 55 are located over the north-western part of the country. High values of HWMId are also diagnosed during the hot season (MAM) for both scenarios. During the rainy season, the ensemble mean of the models projects very strong values of HWMId over a large part of the Senegal especially under the RCP8.5 scenario. The analysis shows that the strongest values of HWMId are expected during the far future (2071-2100) in the country (Figure 8). In fact, during the DJF season, the HWMId values

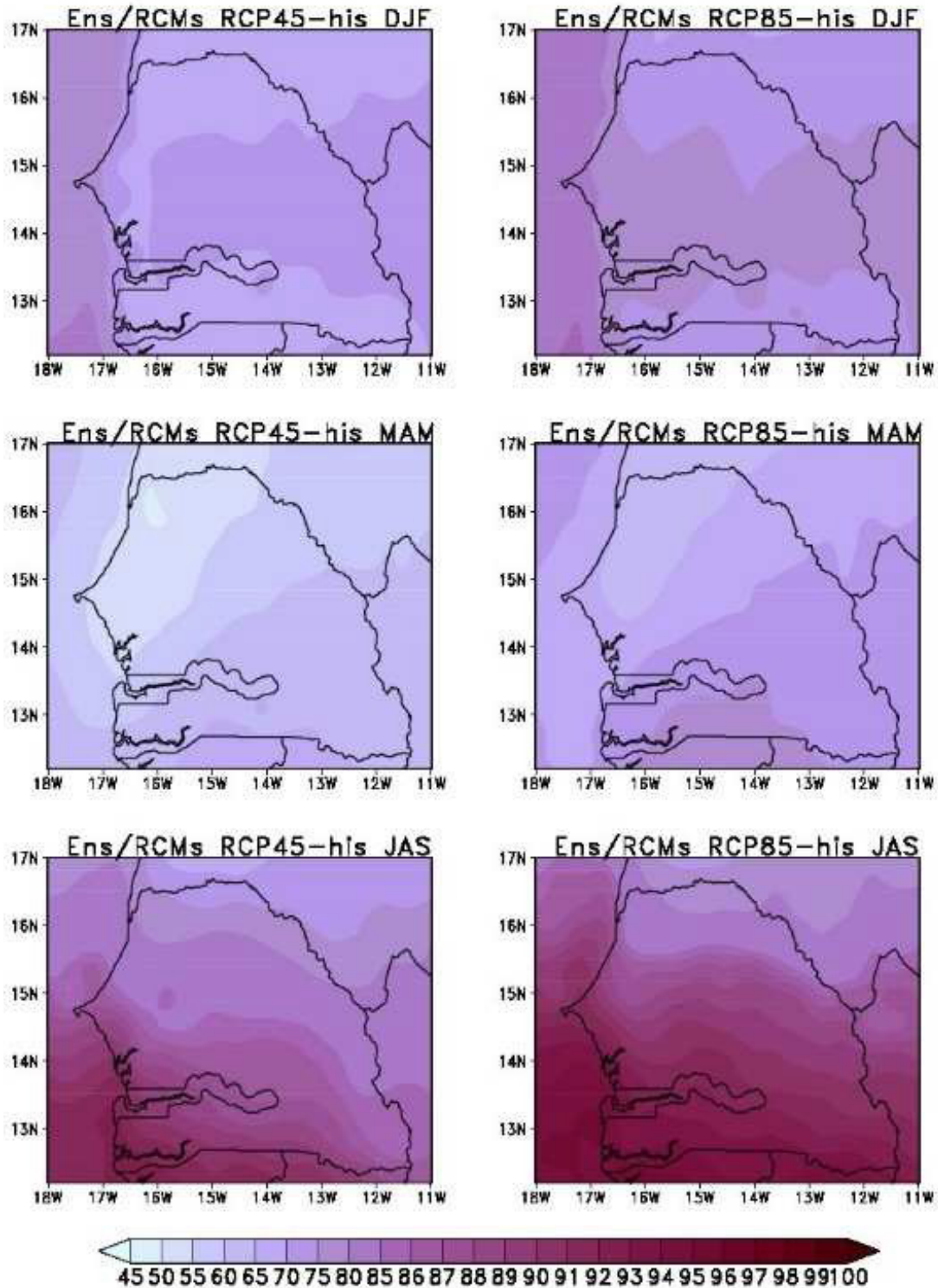


Figure 3. Percentage of days in the near future (2021-2050) with minimum temperature warmer than the 90th percentile of the reference period (1976-2005) during the DJF, MAM and JAS seasons.

can reach 50 and 60, respectively under the RCP4.5 and RCP8.5 scenarios over the north-western part of

the country. These heat waves are relatively important during the hot season for both scenarios with magnitude

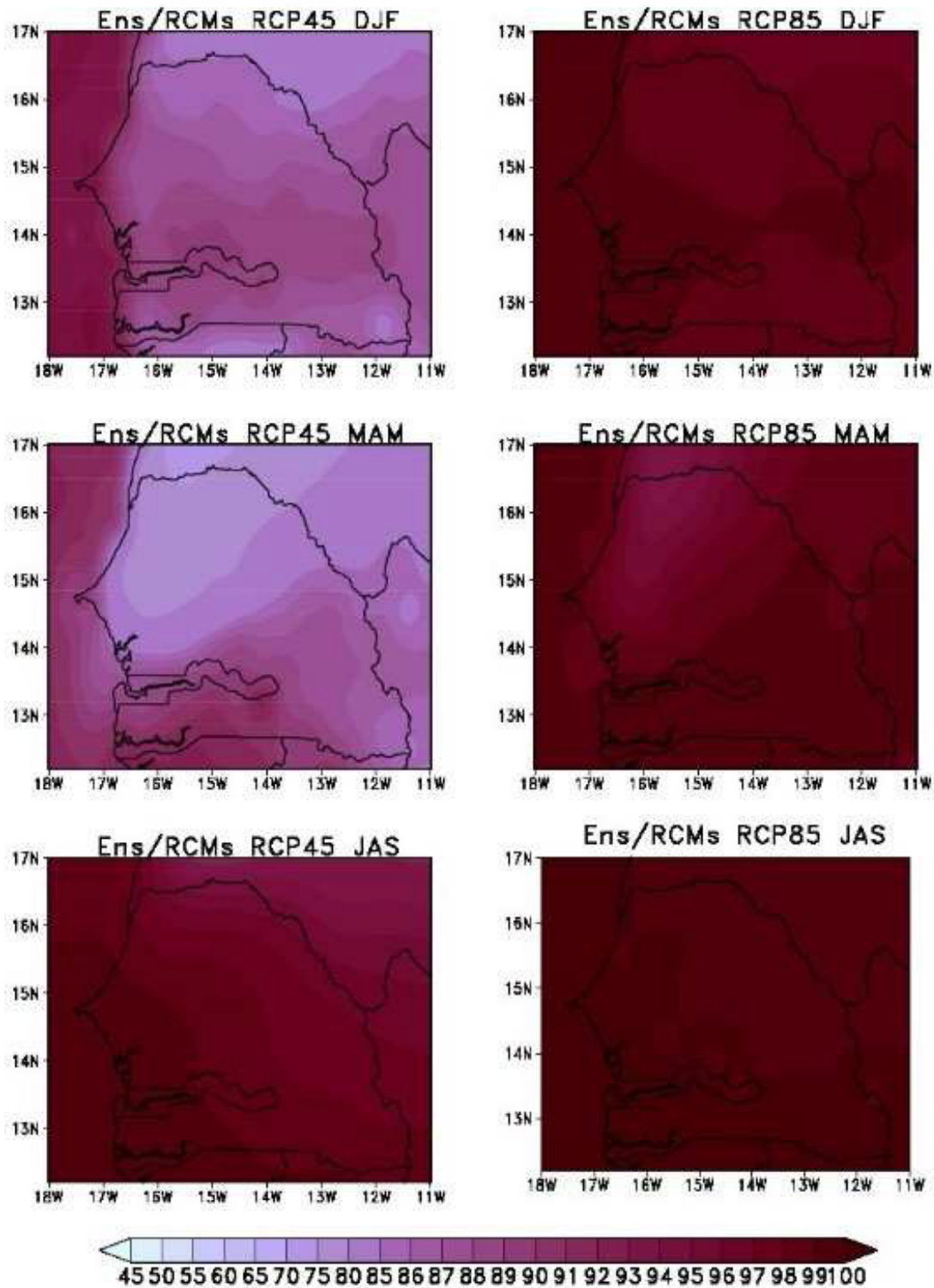


Figure 4. Percentage of days in the far future (2071-2100) with minimum temperature warmer than the 90th percentile of the reference period (1976-2005) during the DJF, MAM and JAS seasons.

exceeding 60 in the western part of the country. The projections obtained with the ensemble mean of the

models during the rainy season (JAS) show that Senegal could be affected by heat waves episodes with

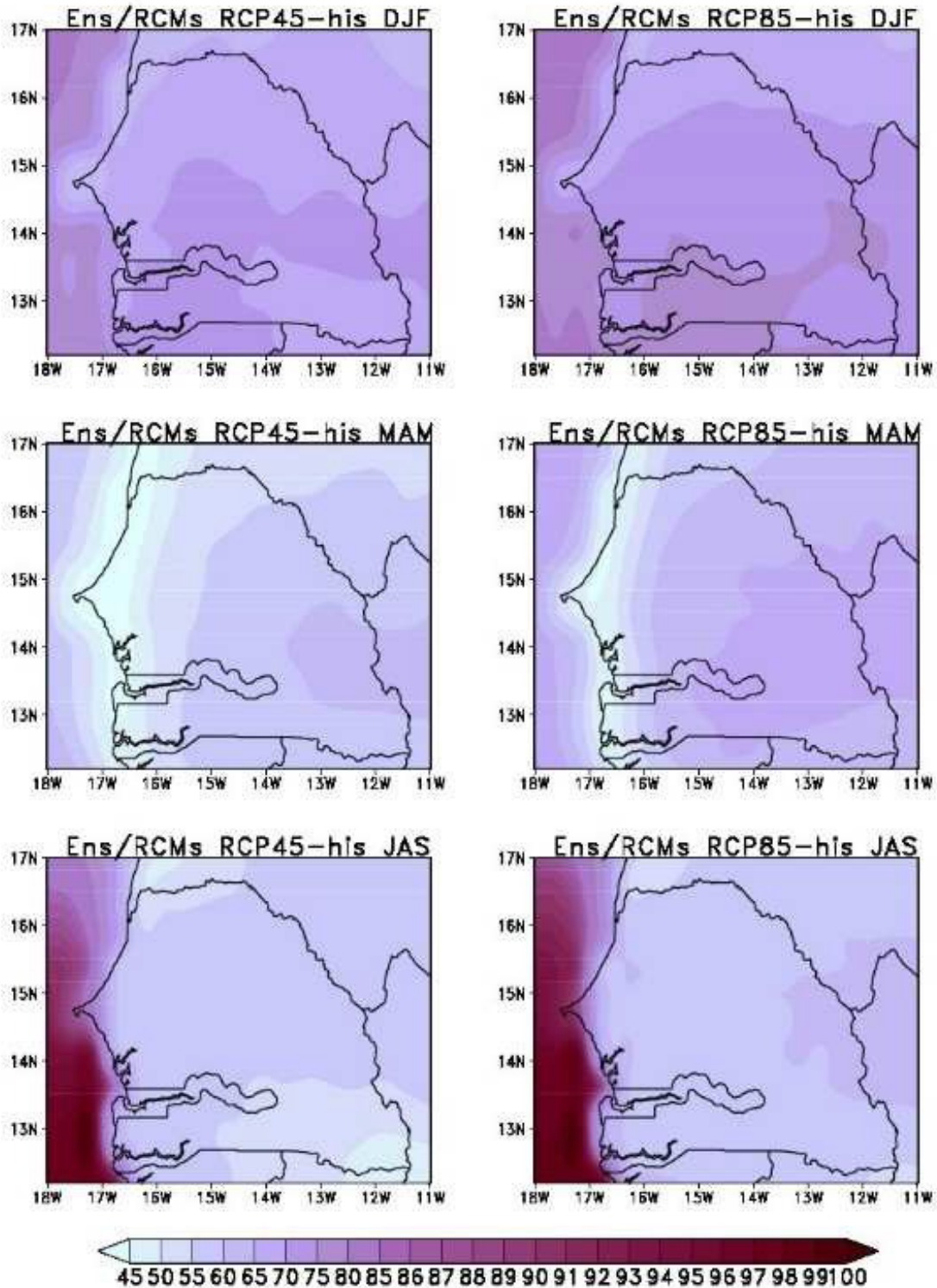


Figure 5. Percentage of days in the near future (2021-2050) with maximum temperature warmer than the 90th percentile of the reference period (1976-2005) during the DJF, MAM and JAS seasons.

magnitudes that could exceed 65 under the severe scenario. This increase of heat waves is consistent with Dosio et al. (2017) studies. This strong increase in

HWMI_d predicted by the ensemble mean of all models during the rainy season (JAS) could be detrimental for agricultural yields during the far future (Sarr and

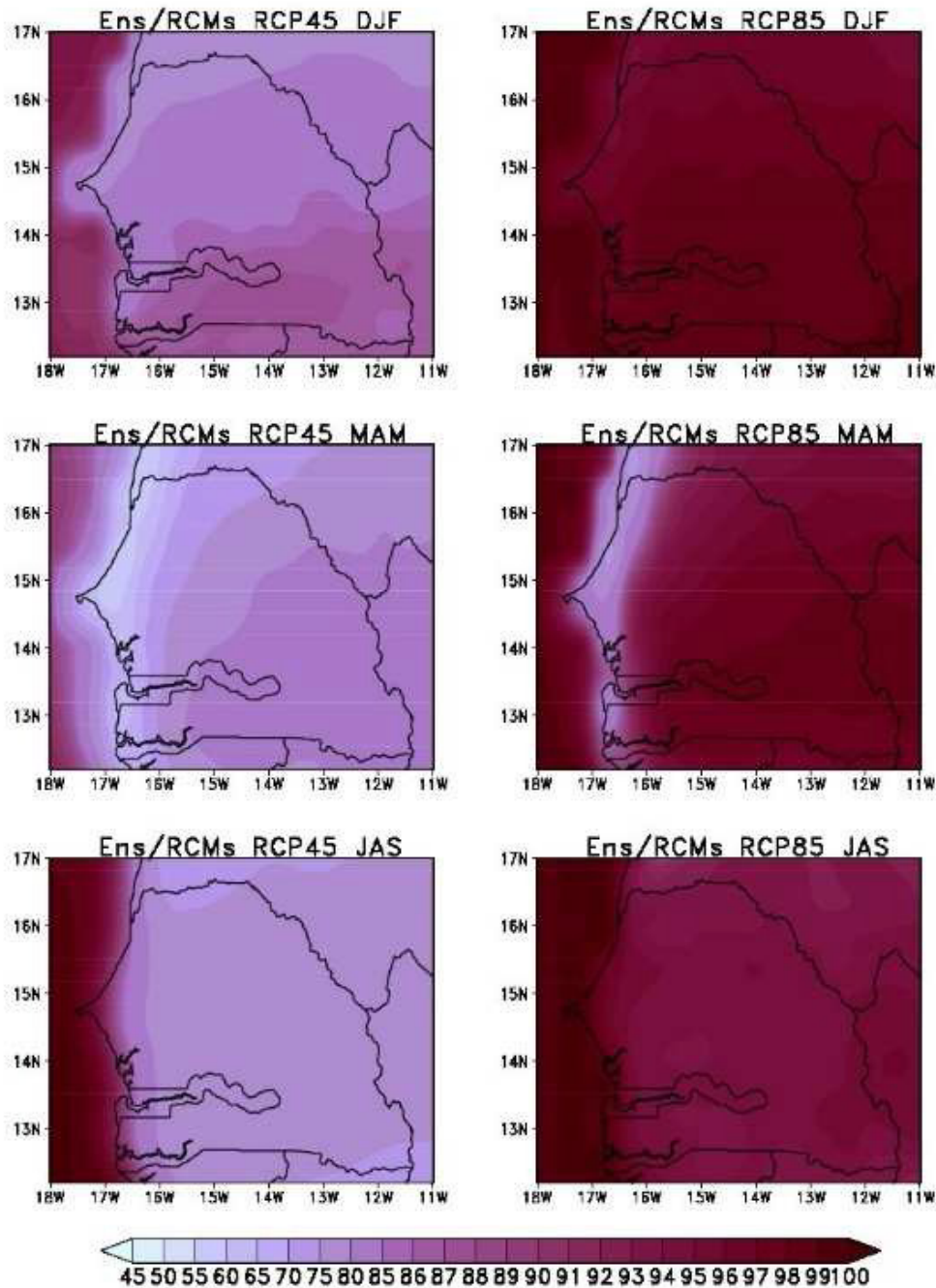


Figure 6. Percentage of days in the far future (2071-2100) with maximum temperature warmer than the 90th percentile of the reference period (1976-2005) during the DJF, MAM and JAS seasons.

Camara, 2018) as well as the health of populations.

The associated health risks

Rising heat waves can negatively impact human health, according to some authors (Campbell et al., 2018;

Hass et al., 2016; Garland et al., 2015). In fact, the combination of temperature and relative humidity increases could have negative impacts on human health. When considering the spatial distribution of the heat index during the reference period (Figure 9), the ensemble mean of the models shows low heat index (HI) values during the cold period (DJF) compared to

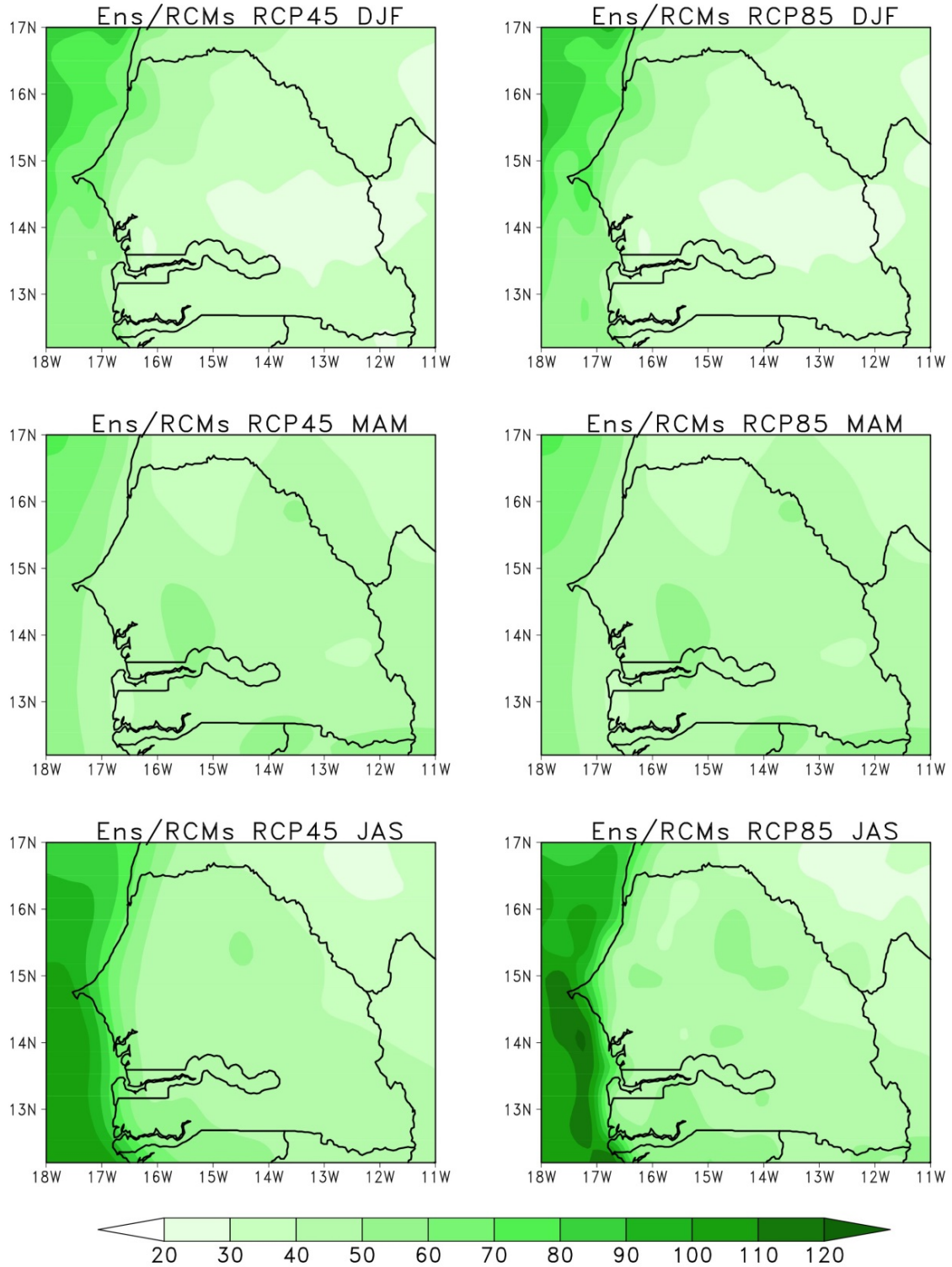


Figure 7. Heat waves magnitude index-daily (HWMId) during the near future (2021-2050) for the DJF, MAM and JAS seasons.

other seasons. The HI is relatively stronger during the hot season (MAM) with values reaching 28°C in Central

and Southern Senegal. The reinforcement of the HI during the hottest season (MAM) may due to the increase in

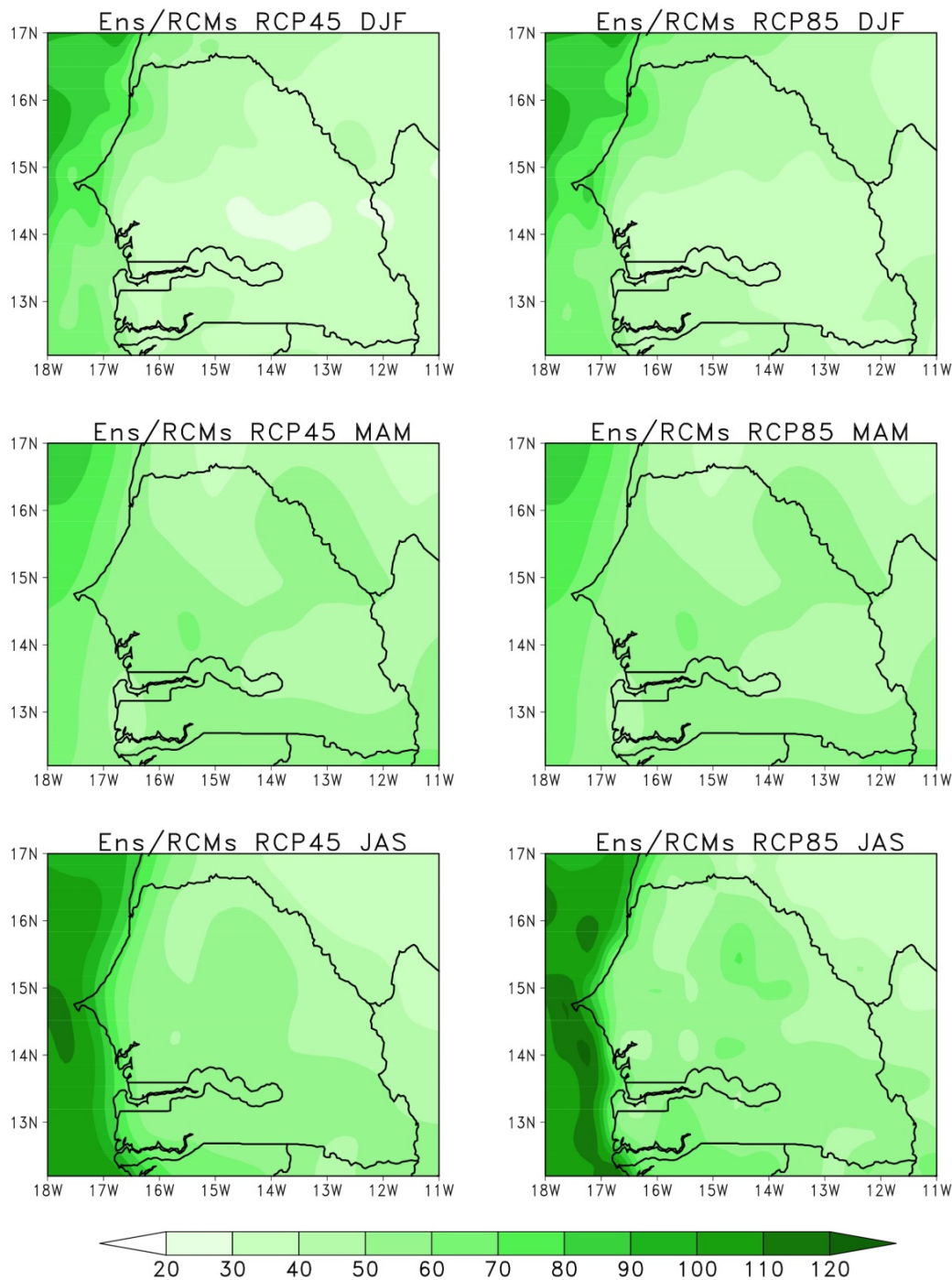


Figure 8. Heat waves magnitude index-daily (HWMId) during the far future (2071-2100) for the DJF, MAM and JAS seasons.

surface temperature. During the rainy season (JAS), the ensemble mean of the models has a North-South gradient with strong HI values located in the north of the country (up to 30°C) as for the surface temperature. This result suggests that the temperature is the main factor controlling the HI spatial variability. These high HI

values obtained during the hot and the rainy seasons correspond to the symptom band I (Table 3). The strong HI values recorded during the rainy season could be due to the increase of the relative humidity during this period. The projections obtained on the heat index during the near future (2021-2050) (Figure 10) show that the

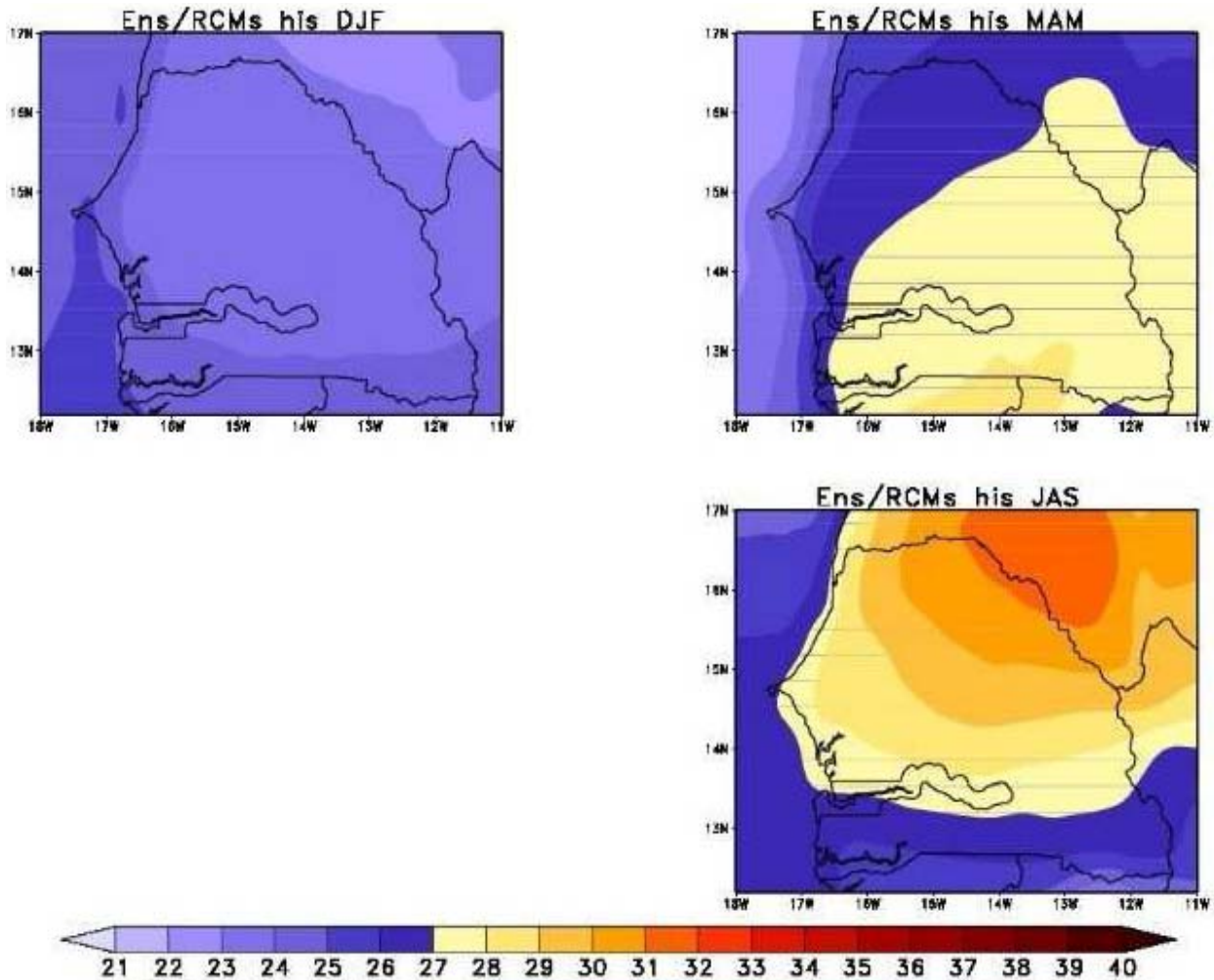


Figure 9. Evolution of heat index (°C) during the reference period (1976-2005) in DJF, MAM and JAS seasons.

Table 3. Heat index threshold and potential health impact.

| Symptom band (SB) | US NWS Classification | Heat index (°C) | Possible adverse effect |
|-------------------|-----------------------|-----------------|--|
| SBI | Caution | 27-32 | Fatigue possible with prolonged exposure and/or physical activity |
| SBII | Extreme caution | 32-39 | Heat stroke, heat cramps, or heat exhaustion possible with prolonged exposure and/or physical activity |
| SBIII | Danger | 39-51 | Heat cramps or heat exhaustion likely, and heat stroke possible with prolonged exposure and/or physical activity |
| SBIV | Extreme danger | > 51 | Heat stroke highly likely |

Source: OHSCO (2008); <http://ggweather.com/101/hi.html>.

ensemble mean of the models presents slight changes during the cold season.

However during the warm season, an increase is noted especially in the south of the country with HI values

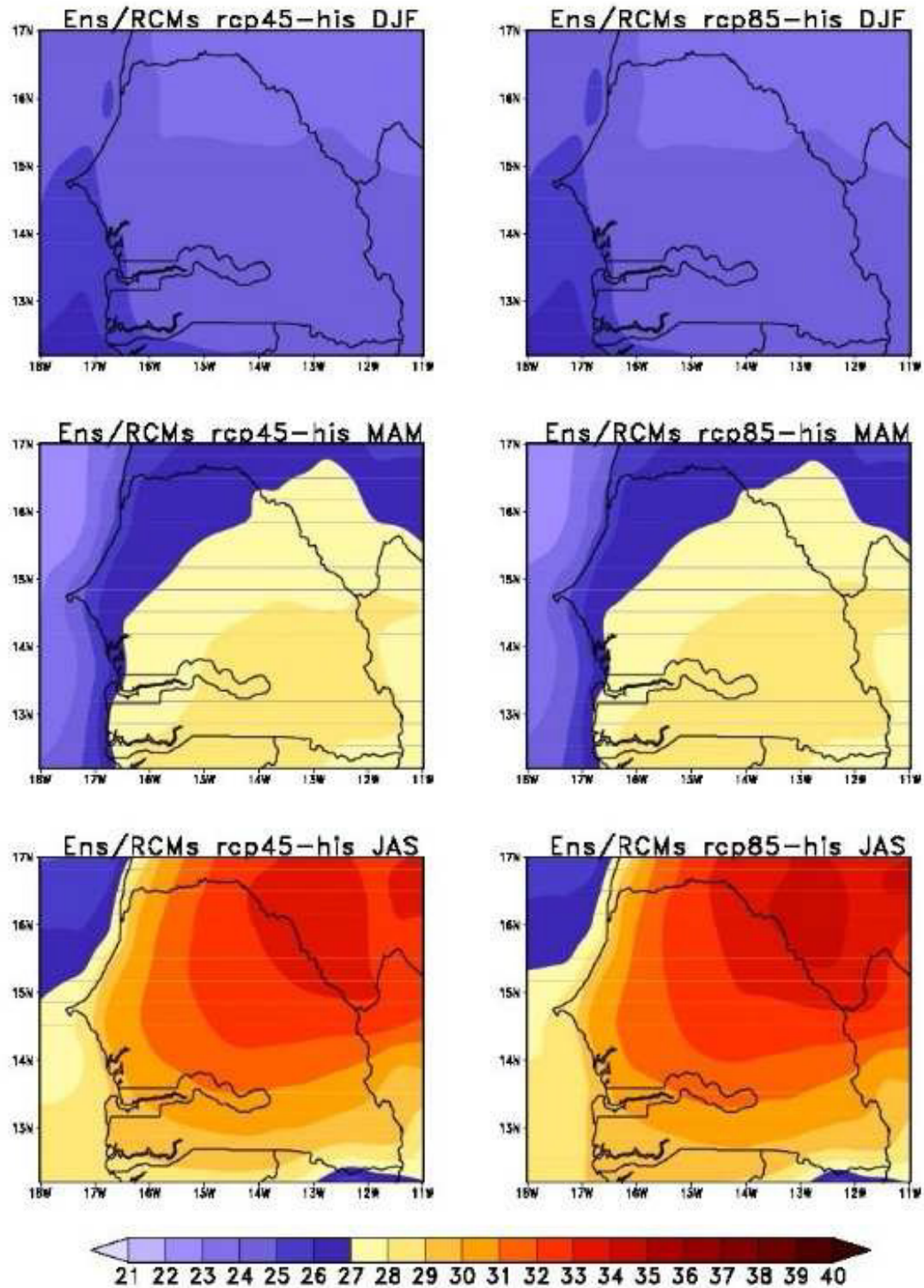


Figure 10. Evolution of the heat index (°C) during the near future (2021-2050) in DJF, MAM and JAS seasons.

greater than 31°C under both scenarios. During the reference period, the highest values are still recorded in

JAS season during the near future (2021-2050). However, the ensemble mean of the models under both

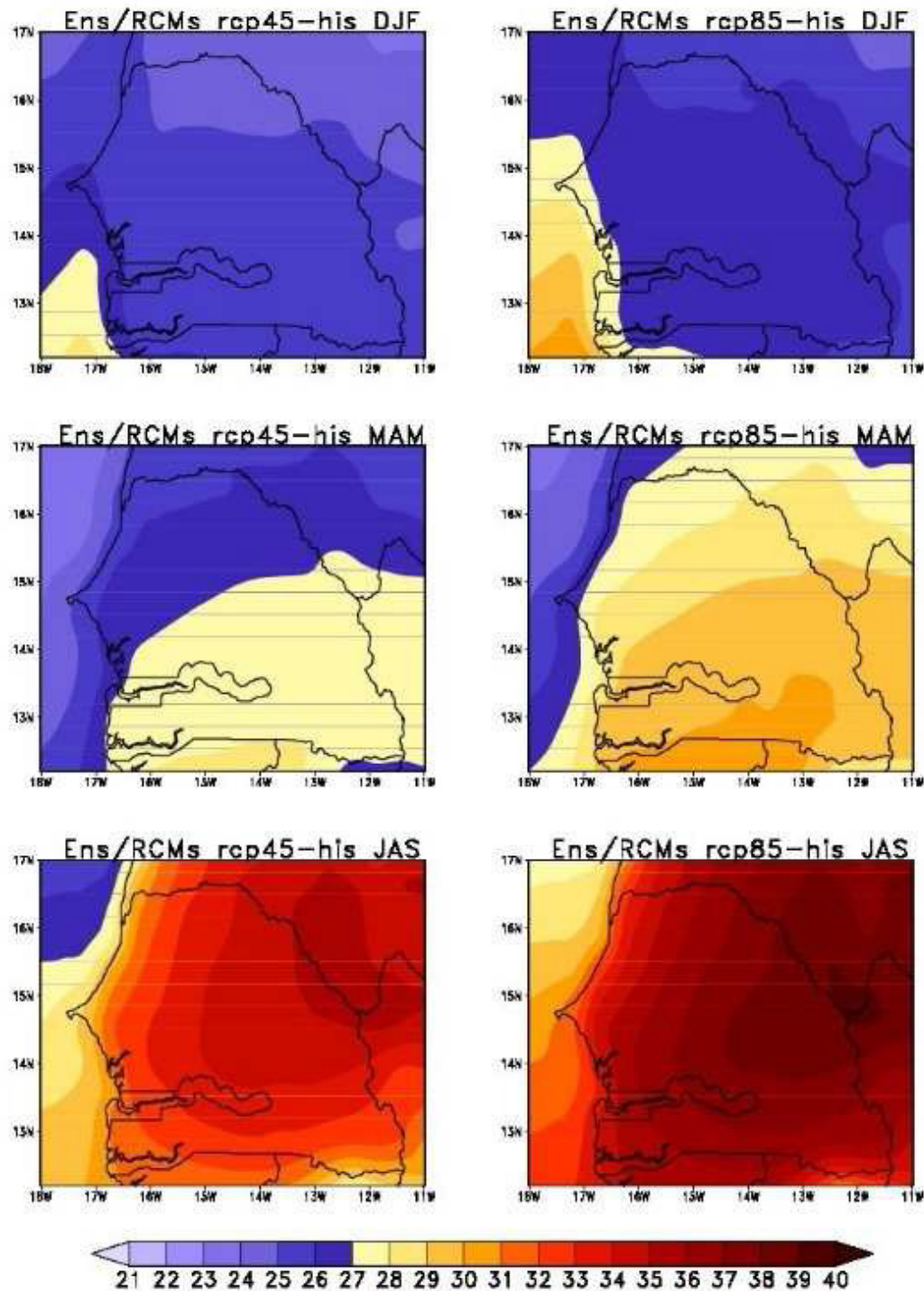


Figure 11. Evolution of the heat index (°C) during the far future (2071-2100) in DJF, MAM and JAS seasons.

scenarios simulates an increase of HI (up to 33°C) in the northeastern part of the country highlighting the presence of the symptom band II (SBII). It should also be noted that this increase in HI values is not always due to an increase in temperature. In fact, relative humidity also

plays a fairly important role, as some studies have shown (Suparta and Yatim, 2017; Hass et al., 2016). Figure 11 shows the projections during the far future (2071-2100) of the heat index. A gradual increase is simulated during this period compared to the reference

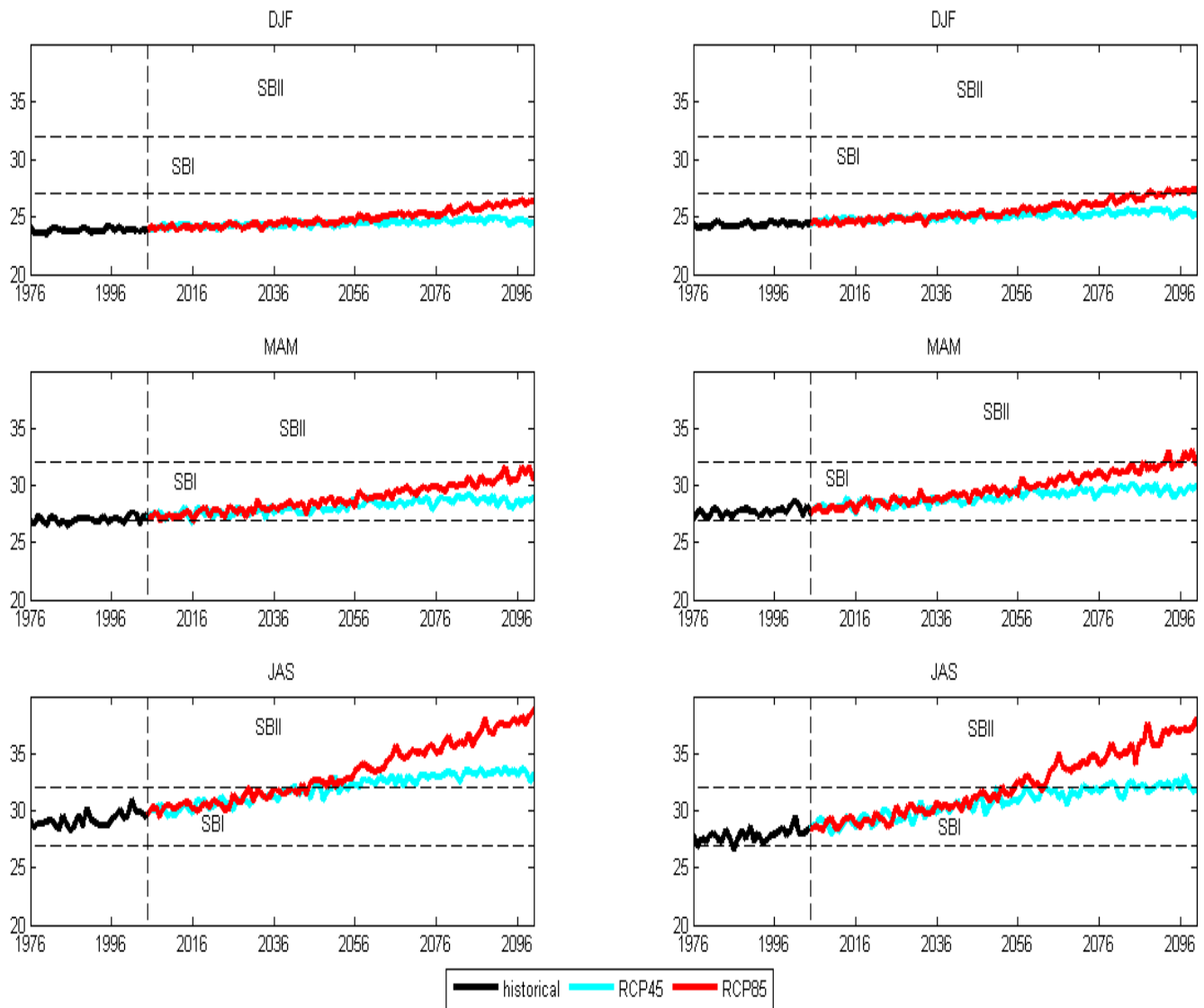


Figure 12. Temporal evolution of the heat index ($^{\circ}\text{C}$) during the cold (DJF), hot (MAM) and wet seasons (JAS) in the north (left panel) and in the south (right panel) of Senegal.

period and the near future. However, this increase is generally less than the threshold value (27°C) in DJF. It is only on the southwest coast of Senegal that HI values of around 27°C are recorded under the RCP8.5 scenario.

In MAM, the ensemble mean of the models simulates a slight decrease under the RCP4.5 scenario compared to the near future. However, under the RCP8.5 scenario, it simulates an important increase compared to the near future (2021-2025) with values greater than 32°C corresponding to the symptom II band ($32^{\circ}\text{C} < \text{SBII} < 41^{\circ}\text{C}$). The situation could be much more alarming during the rainy season (JAS) due to the strong increase of humidity. In fact, the projections obtained with the ensemble mean of the models by 2100 shows HI values which are generally above 27°C under both

scenarios across the country. Under the RCP4.5 scenario, it highlights the presence of symptom band I in the western part of the country and the presence of symptom band II in the south-east of the country. However, under the RCP8.5 scenario, a large increase in symptom band II is expected almost all over Senegal, causing serious discomfort (fatigue, heat stroke, heat cramps, etc.) for local populations.

The temporal evolution of the seasonal heat index in Northern ($17^{\circ}\text{W}-12^{\circ}\text{W}$, $14.4^{\circ}\text{N}-16.8^{\circ}\text{N}$) and Southern ($17^{\circ}\text{W}-12^{\circ}\text{W}$, $12.7^{\circ}\text{N}-14.4^{\circ}\text{N}$) Senegal from 1976 to 2100 is as shown in Figure 12. The heat index has increased in almost all parts of Senegal. However, this increase is relatively low during the cold season (DJF). However, the HI values may reach the SBI at the end of the

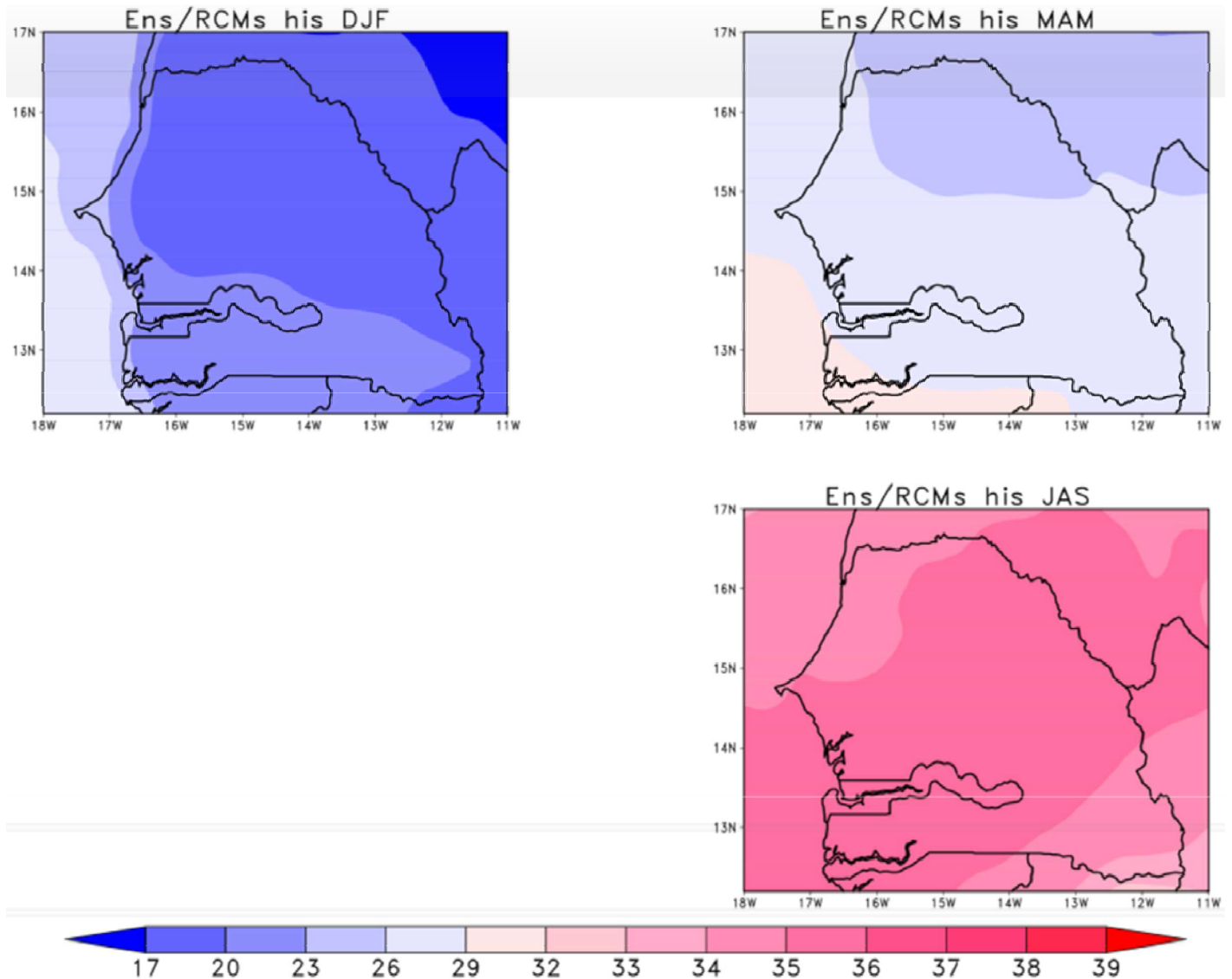


Figure 13. Evolution of the humidex ($^{\circ}\text{C}$) during the reference period (1976-2005) in DJF, MAM and JAS seasons.

century under the RCP8.5 scenario in coherence with the temperature rise in the far future Appendix Figures 6 and 7. During the hot season (MAM), the ensemble mean of the models shows that the HI values are relatively stronger compared to cold season. The HI values are also stronger in the south and can reach the SBII under the RCP8.5 scenario. A strong increase of HI values is recorded during the rainy season compared to other seasons causing serious discomfort to the local populations. The presence of SBII is highlighted by the ensemble mean of the models in the north and the center of country from 2050 for both scenarios. This increase is relatively low in the south of the country. It reaches the SBII from 2070 only for the RCP8.5 scenario. This large increase in the heat index could be harmful for those working or exercising physical activity.

As for the heat index, the evolution of humidex during the reference period (Figure 13) shows that the cold season (DJF) is the more comfortable season followed by the hot season (MAM). However, some discomfort (category B) is observed during this season particularly in the south-west of the country. In fact, some discomfort are observed in all the country. The projections during the near future (2021-2050) of the humidex are as shown in the Figure 14. The results show a slight increase of the category B during the hot season in the south of the country and in all the country during the rainy season under both scenarios. Compared to heat index, the results obtained during the hot season (MAM) show that when we consider the humidex the heat stress would not affected the human health during this season. Figure 15 shows the evolution of the

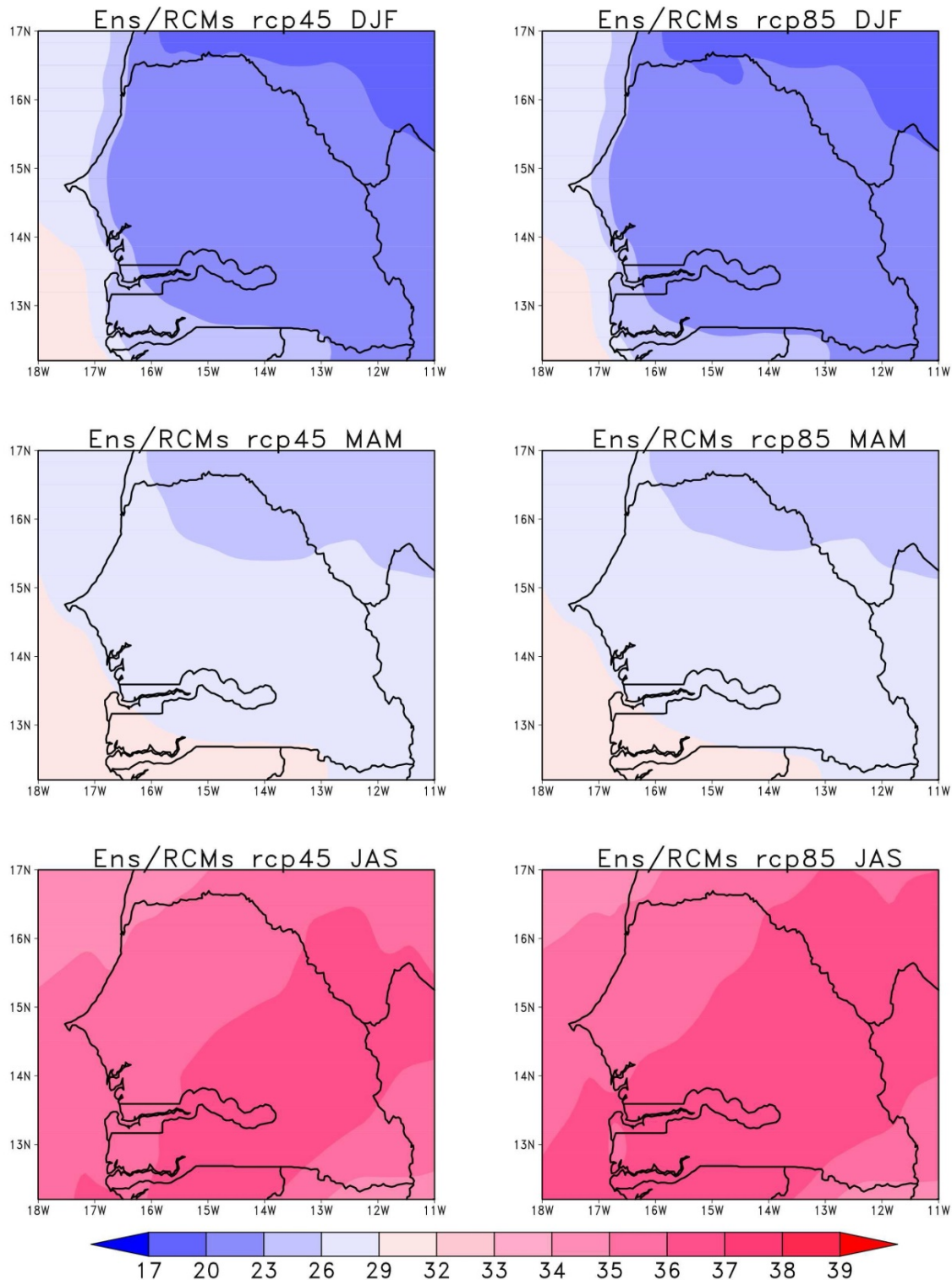


Figure 14. Evolution of the humidex during the near future (2021-2050) in DJF, MAM and JAS seasons.

humidex during the far future (2071-2100). Results show that the human discomfort during this period is imminent. In fact, the category B continues to increase

and its presence is noted during the cold season in the south of the country particularly under the RCP8.5 scenario. Admittedly, the acclimatization capacity of

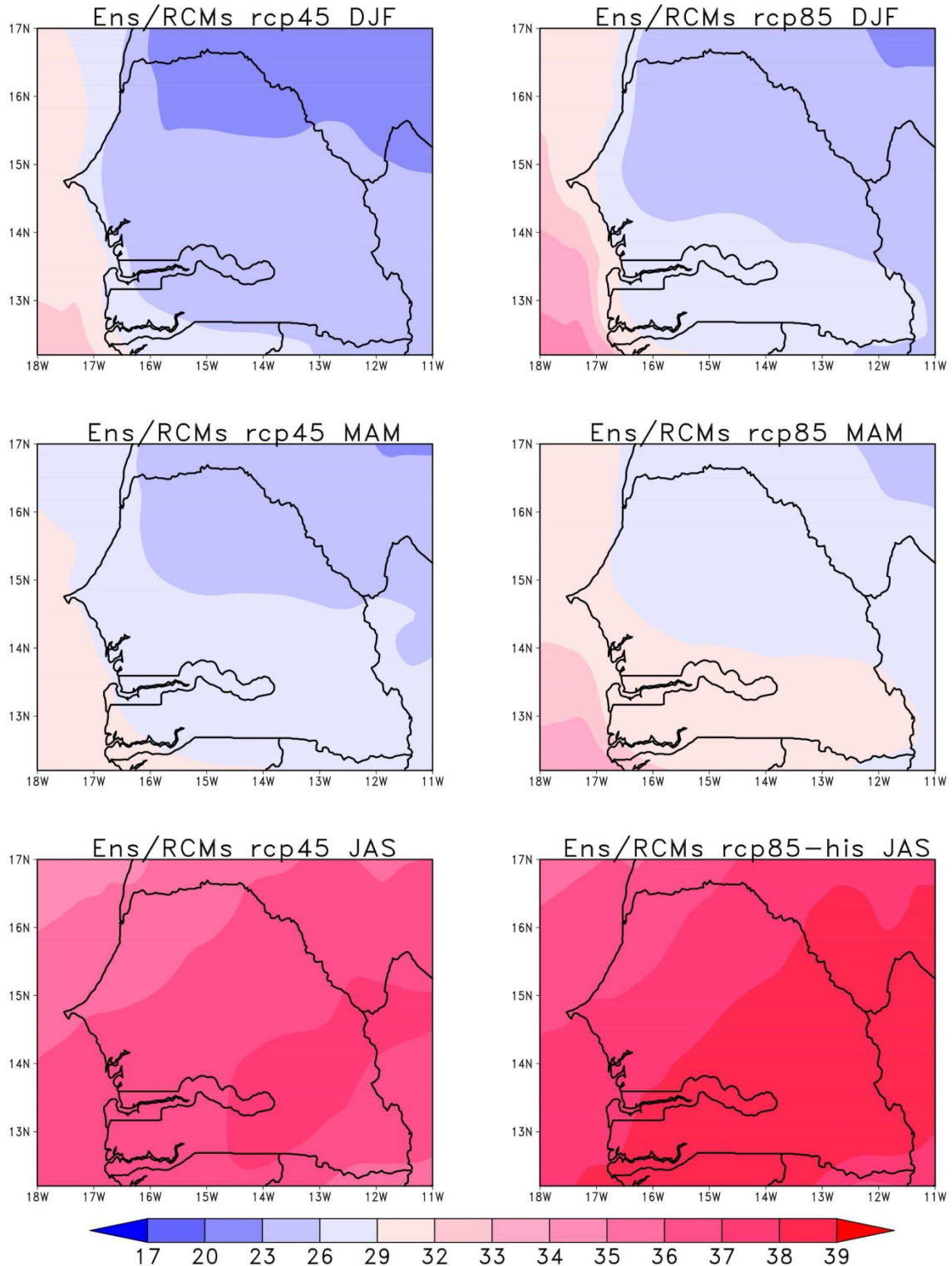


Figure 15. Evolution of the humidex during the far future (2071-2100) in DJF, MAM and JAS seasons.

the human body in the country of residence to global warming is not well studied, especially in the countries of the world. However, in Sahel regions for example,

large temperature increases combined with strong humidity could be mortal particularly for the sick, the small children and the elderly persons.

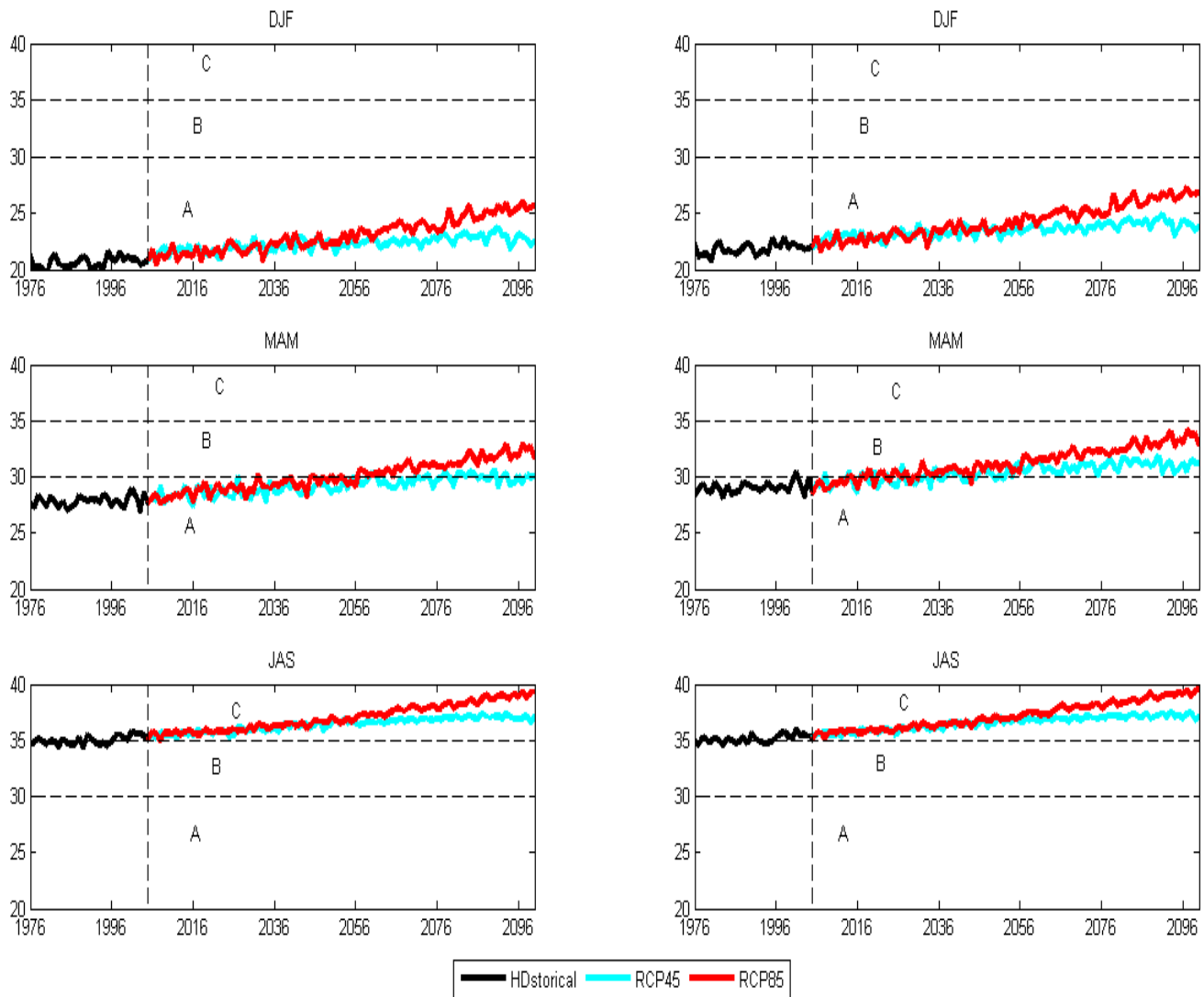


Figure 16. Temporal evolution of the humidex ($^{\circ}\text{C}$) during the cold (DJF), hot (MAM) and wet seasons (JAS) in the north (left panel) and in the south (right panel) of Senegal.

The temporal evolution of the seasonal humidex in Senegal from 1976 to 2100 are shown in Figure 16 for the north ($17^{\circ}\text{W}-12^{\circ}\text{W}$, $14.4^{\circ}\text{N}-16.8^{\circ}\text{N}$) and the south ($17^{\circ}\text{W}-12^{\circ}\text{W}$, $13.7^{\circ}\text{N}-14.4^{\circ}\text{N}$). The results show that the presence of category A during the cold season (DJF) which is characterized by a little or no discomfort in the south and the north of the country. However, the humidex values are stronger in the south with values which can reach 27°C for RCP8.5 scenario. During the hot season (MAM), the ensemble mean of the models shows the presence of the category B, characterized by some discomfort from 2060 in the north for only the RCP8.5 and in the south for both scenarios. The strong humidex values are recorded during the wet season (JAS) in the north and south of the country highlighting the development of the category C Table 4.

CONCLUSION AND PERSPECTIVES

In this study, the ensemble mean of 5 CORDEX RCMs was considered to analyze the seasonal evolution (DJF, MAM and JAS) of the mean temperature as well as some extreme temperatures such as Tn90p (percentage of warm nights), Tx90p (percentage of hot days) and heat waves during the near future (2021-2050) and the far future (2071-2100). The biases of the ensemble mean of the models considered were first assessed. The validation step results highlight the good performance of the ensemble mean of the models. The latter was then considered in the study of the future evolution of temperature and extreme temperature events. An increase in temperature is predicted by the ensemble mean of the models across the country. The

Table 4. Humidex threshold and potential health impacts.

| Categories corresponding to the rising thermal discomfort conditions | Humidex (°C) | Impacts |
|--|--------------|--------------------------------------|
| A | 30 | Little or no discomfort |
| B | 30-34 | Noticeable discomfort |
| C | 35-39 | Evident discomfort |
| D | 40-45 | Intense discomfort; avoid exertion |
| E | 54 | Real dangerous; heat stroke probable |

Source: NIOSH (1992); <http://www.hpc.ncep.noaa.gov/html/heatindex.shtml>.

highest increases are recorded during the DJF season and can reach 1.5°C under the RCP8.5 scenario over most of the country soon. During the far future, increases can reach 2 and 4.5°C, respectively under the scenarios RCP4.5 and RCP8.5. The warming is relatively lower during the rainy season (JAS) compared to DJF and MAM.

For extreme temperature events, the largest increases in warm nights are located during the DJF season in the south of the country for both scenarios with Tn90p occurrences higher than 70% by 2050. During the far future, the increase is above 80% over a large part of the country. These increases are more significant during the JAS season under the RCP8.5 scenario with Tn90p values close to 100% over a large part of the country and this could have negative consequences on the agriculture of our country. Changes in the percentage of hot days (Tx90p) are relatively lower than those of Tn90p almost nationwide. The largest increases in Tx90p in the near future are recorded in DJF under the RCP8.5 scenario and are less than 70%. By 2100, the Tx90p maxima recorded during the DJF season in the southern zone of the country can reach 94 and 98.5% respectively under the RCP4.5 and RCP8.5 scenarios. The heat wave magnitude index-daily analysis (HWMId) shows that the magnitude of the heat waves are stronger during the hot and the rainy season with values exceeding 50 over most parts of the country during the far future.

To study the impact of this heat stress on human health, we analyzed the heat index and the humidex. The results obtained show that maxima of heat index corresponding to symptom band II are recorded in JAS over the south-east of the country during the near future and over most part of the country during the far future for both scenarios. In addition, the frequency of the symptom band II is higher during this season. The analysis of the humidex shows an increase of the discomfort which is more pronounced during the rainy season.

Finally, these results show that temperatures could become stronger in Senegal in the future, resulting in longer and more frequent heat waves. This warming could have negative consequences for the natural ecosystem and local populations. In perspective, it would be

important to conduct additional studies to better quantify the impact of this future warming on socio-economic activities of the population in order to put in place appropriate adaptation measures.

ABBREVIATIONS

DJF, Average from December to February; **MAM**, average from March to May; **JAS**, average from July to September; **CORDEX**, Coordinated Regional climate Downscaling Experiment (CORDEX) program; **CRU**, Climate Research Unit.

CONFLICT OF INTERESTS

The authors have not declared any conflict of interests.

ACKNOWLEDGEMENTS

This research paper was supported by the Assane SECK University of Ziguinchor (UASZ) and the "Fonds d'Impulsion de la Recherche Scientifique (FIRST) du MESRI/Senegal".

REFERENCES

- Anderson GB, Bell ML, Peng R (2013). Methods to Calculate the Heat Index as an Exposure Metric in Environmental Health Research. *Environmental Health Perspectives* 121(10):1111-1119.
- Baldauf M, Seifert A, Förstner J, Majewski D, Raschendorfer M, Reinhardt T (2011). Operational convective-scale numerical weather prediction with the COSMO model: description and sensitivities. *Monthly Weather Review* 139(12):3887-3905.
- Basak JK, Titumir RA, Biswas JK, Mohinuzzaman M (2013). Impacts of Temperature and Carbon dioxide on Rice yield in Bangladesh. *Bangladesh Rice Journal* 17(1-2):15-25.
- Boko M, Niang I, Nyong A, Vogel C, Githeko A, Medany M, Osman-Elasha B, Tabo R, Yanda P (2007). Africa Climate Change: impacts, adaptation and vulnerability. In ML Parry, OF Canziani, JP Palutikof, PJ van der Linden, & CE Hanson (Eds.), *Contribution of Working Group II to the Fourth Assessment Report of the Intergovernmental Panel on Climate Change*. Cambridge, UK: Cambridge University Press, pp. 433-467.
- Camara M, Diedhiou A, Sow BA, Diallo MD, Diatta S, Mbaye I, Diallo I

- (2013). Analyse de la pluie simulée par les modèles climatiques régionaux de CORDEX en Afrique de l'Ouest. *Science et changements planétaires/Sécheresse* 24(1):14-28.
- Campbell S, Remenyi TA, White CJ, Johnston FH (2018). Heatwave and health impact research: A global review. *Health and Place* 53:210-218.
- Ceccherini G, Russo S, Ameztoy I, Marchese AF, Carmona-Moreno C (2017). Heat waves in Africa 1981–2015, observations and reanalysis. *Natural Hazards and Earth System Sciences* 17(1):115-125.
- CEDEAO-ClubSahel/OCDE/CILSS Climate and Climate Change (2008). The Atlas on Regional Integration in West Africa Environment Series, p.13. "<http://www.oecd.org/fr/csao/publications/40121057.pdf>"
- Christensen OB, Drews M, Christensen JH (2006). The DMI-HIRHAM regional climate model version 5, Denmark: DMI Tech. Rep. 06-17.
- Diallo I, Giorgi F, Deme A, Tall M, Mariotti L, Gaye AT (2016). Projected changes of summer monsoon extremes and hydroclimatic regimes over West Africa for the twenty-first century. *Climate dynamics* 47(12):3931-3954.
- Dosio A (2017). Projection of temperature and heat waves for Africa with an ensemble of CORDEX Regional Climate Models. *Climate Dynamics* 49(1-2):493-519.
- Garland R, Matooane M, Engelbrecht F, Bopape MJ, Landman W, Naidoo M, Merwe J, Wright C (2015). Regional projections of extreme apparent temperature days in Africa and the related potential risk to human health. *International Journal of Environmental Research and Public Health* 12(10):12577-12604.
- Gbobaniyi E, Sarr A, Sylla MB, Diallo I, Lennard C, Dosio A, Dhiédiou A, Kamga A, Klutse NA, Hewitson B, Nikulin G (2014). Climatology, annual cycle and interannual variability of precipitation and temperature in CORDEX simulations over West Africa. *International Journal of Climatology* 34(7):2241-2257.
- Giorgi F, Jones C, Asrar G (2009). Addressing climate information needs at the regional level. The CORDEX framework. WMO Bulletin, July 2009 issue.
- Giorgi F, Coppola E, Raffaele F, Diro GT, Fuentes-Franco R, Giuliani G, Mangain A, Llopart MP, Mariotti L, Torma C (2014). Changes in extremes and hydroclimatic regimes in the CREMA ensemble projections. *Climatic Change* 125(1):39-51.
- Hass A, Ellis K, Reyes Mason L, Hathaway J, Howe D (2016). Heat and humidity in the city: neighborhood heat index variability in a mid-sized city in the southeastern United States. *International Journal of Environmental Research and Public Health* 13(1):117.
- Hayhoe K, Sheridan S, Kalkstein L, Greene S (2010). Climate change, heat waves, and mortality projections for Chicago. *Journal of Great Lakes Research* 36:65-73.
- Hulme M, Doherty R, Ngara T, New M, Lister D (2001). African climate change: 1900-2100. *Climate research* 17(2):145-168.
- IPCC (2013). *Climate Change. The Physical Science Basis*. In TF. Stocker, Qin D, Plattner GK, M. Tignor, SK. Allen, J. Boschung, A. Nauels, Xia Y, Bex V & Midgley PM (Eds.), *Contribution of Working Group I to the Fifth Assessment Report of the Intergovernmental Panel on Climate Change* (p. 1535). Cambridge, United Kingdom and New York, NY, USA: Cambridge University Press.
- Jacob D, Bärring L, Christensen OB, Christensen JH, De Castro M, Deque M, Giorgi F, Hagemann S, Hirschi M, Jones R, Kjellström E (2007). An inter-comparison of regional climate models for Europe: model performance in present-day climate. *Climatic Change* 81(1):31-52.
- Kim J, Waliser DE, Mattmann CA, Goodale CE, Hart AF, Zimdars PA, Crichton DJ, Jones C, Nikulin G, Hewitson B, Jack C (2014). Evaluation of the CORDEX-Africa multi-RCM hindcast: systematic model errors. *Climate dynamics* 42(5-6):1189-11202.
- Kotir JH (2011). Climate change and variability in Sub-Saharan Africa: a review of current and future trends and impacts on agriculture and food security. *Environment, Development and Sustainability* 13(3):587-605.
- Laprise R, Hernández-Díaz L, Tete K, Sushama L, Šeparović L, Martynov A, Winger K, Valin M (2013). Climate projections over CORDEX Africa domain using the fifth-generation Canadian Regional Climate Model (CRCM5). *Climate Dynamics* 41(11-12):3219-3246.
- Ly M, Traoré SB, Alhassane A, Sarr B (2013). Evolution of Some Observed Climate Extremes in the west African Sahel. *Weather and Climate Extreme* 1:19-25.
- Mariotti L, Diallo I, Coppola E, Giorgi F (2014). Seasonal and intraseasonal changes of African monsoon climates in 21st century CORDEX projections. *Climatic Change* 125(1):53-65.
- van Meijgaard E, van Uffl L, van de Berg WJ, Bosveld FC, van den Hurk B, Lenderink G, Siebesma AP (2008). The KNMI regional atmospheric climate model RACMO version 2.1, Tech. Rep. 302.
- Moron V, Oueslati B, Pohl B, Rome S, Janicot S (2016). Trends of mean temperatures and warm extremes in northern tropical Africa (1961-2014) from observed and PPCA-reconstructed time series. *Journal of Geophysical Research: Atmospheres* 121(10):5298-319.
- Moss RH, Edmonds JA, Hibbard KA, Manning MR, Rose SK, van Vuuren DP, Carter TR, Emori S, Kainuma M, Kram T, Meehl GA, Mitchell JF, Nakicenovic N, Riahi K, Smith SJ, Stouffer RJ, Thomson AM, Weyant JP, Wilbanks TJ (2010). The next generation of scenarios for climate change research and assessment. *Nature* 463:747-756.
- New M, Hewitson B, Stephenson DB, Tsiga A, Kruger A, Manrique A, Gomez B, Coelho CAS, Masisi DN, Kululanga E, Mbambalala E, Adesina F, Saleh H, Kanyanga J, Adosi J, Bulane L, Fortunata L, Mdoka ML and Lajoie R (2006). Evidence of Trends in Daily Climate Extremes over Southern and West Africa. *Journal of Geophysical Research* 111:1-11.
- Nikulin G, Jones C, Giorgi F, Asrar G, Büchner M, Cerezo-Mota R, Christensen OB, Déqué M, Fernandez J, Hänsler A, van Meijgaard E (2012). Precipitation climatology in an ensemble of CORDEX-Africa regional climate simulations. *Journal of Climate*. 25(18):6057-6078.
- Niosh (1992). Recommendations for occupational safety and health: compendium of policy documents and statements. Department of Health and Human Services, Public Health Service, Centers for Disease Control and Prevention, National Institute for Occupational Safety and Health, DHHS (NIOSH) Publication No. 92-100. <http://www.hpc.ncep.noaa.gov/html/heatindex.shtml>.
- Occupational Health and Safety Council of Ontario (OHSCO) (2008). <http://ggweather.com/101/hi.htm>.
- SAGNA P (2000) : 0A P.y.ificer.com/101/hi Atlas du Sénégal, Paris, s du Saris, , 101/hi.htm/101
- Salack S, Sarr B, Sangare SK, Ly M, Sanda IS, Kunstmann H (2015). Crop-climate ensemble scenarios to improve risk assessment and resilience in the semi-arid regions of West Africa. *Climate Research* 65:107-121.
- Samuelsson P, Jones CG, Will' En U, Ullerstig A, Gollvik S, Hansson UL, Jansson E, Kjellström M C, Nikulin G, Wyser K (2011). The Rossby Centre Regional Climate model RCA3: model description and performance. *Tellus A: Dynamic Meteorology and Oceanography* 63(1):4-23.
- Sarr AB, Camara M (2017). Evolution des indices pluviométriques extrêmes par l'analyse de modèles climatiques régionaux du programme CORDEX: Les projections climatiques sur le Sénégal. *European Scientific Journal* 13:17.
- Sarr AB, Camara M (2018). Simulation of the impact of climate change on peanut yield in Senegal. *International Journal of physical Sciences* 13(5):79-89.
- Suparta W, Yatim AN (2017). An analysis of heat wave trends using heat index in East Malaysia. In *Journal of Physics: Conference Series* 852(1):012005. IOP Publishing.
- Sylla MB, Nikiema PM, Gibba P, Kebe I, Klutse NA (2016). Climate change over West Africa: Recent trends and future projections. In *Adaptation to climate change and variability in rural West Africa*, Springer, Cham, pp. 25-40.
- Willett KM, Sherwood S (2012). Exceedance of heat index thresholds for 15 regions under a warming climate using the wet-bulb globe temperature. *International Journal of Climatology* 32(2):161-177.

APPENDIX FIGURES

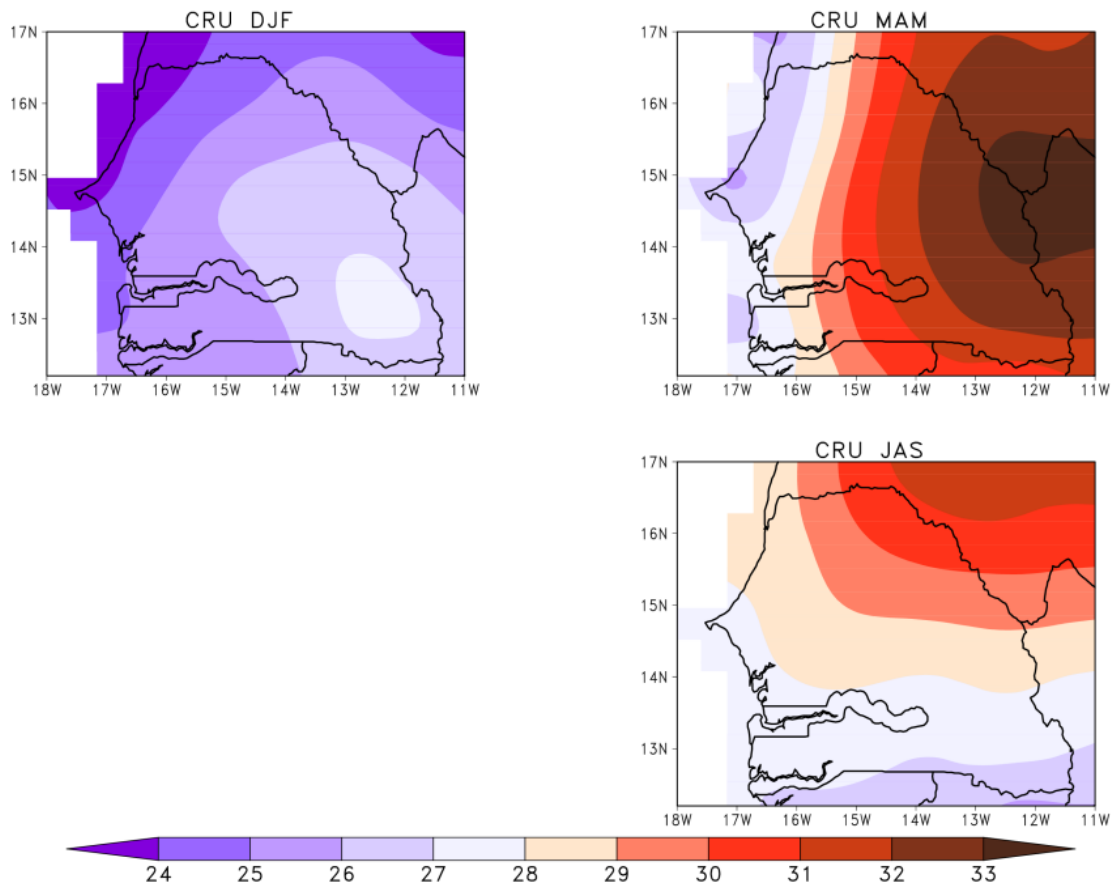


Figure 1. Mean temperature in DJF, MAM and JAS seasons from 1989 to 2008 for CRU data.

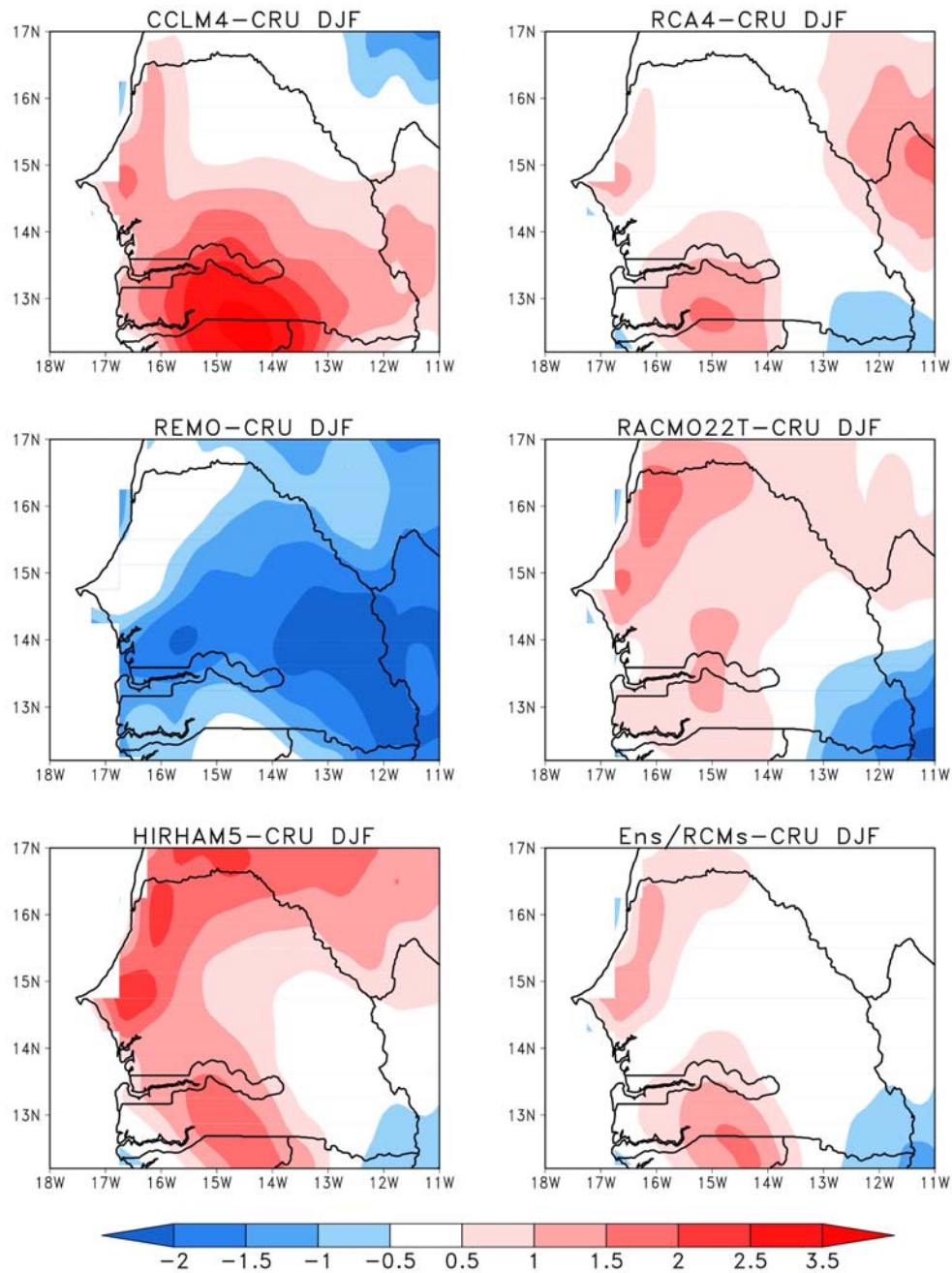


Figure 2. Deviation from CRU observations of mean DJF temperature averaged from 1989 to 2008 of the RCMs and their ensemble mean.

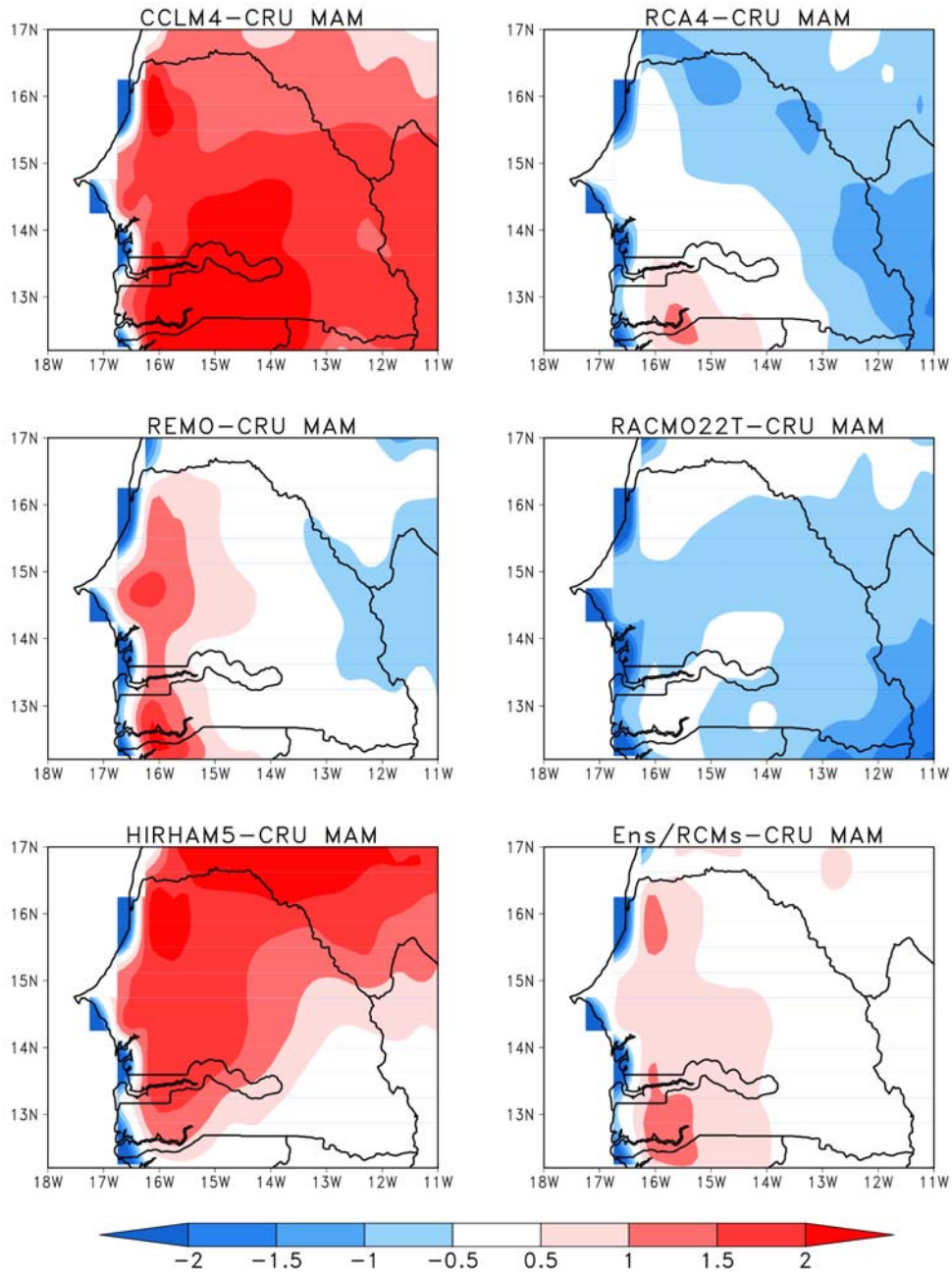


Figure 3. Deviation from CRU observations of mean MAM temperature averaged from 1989 to 2008 of the RCMs and their ensemble mean.

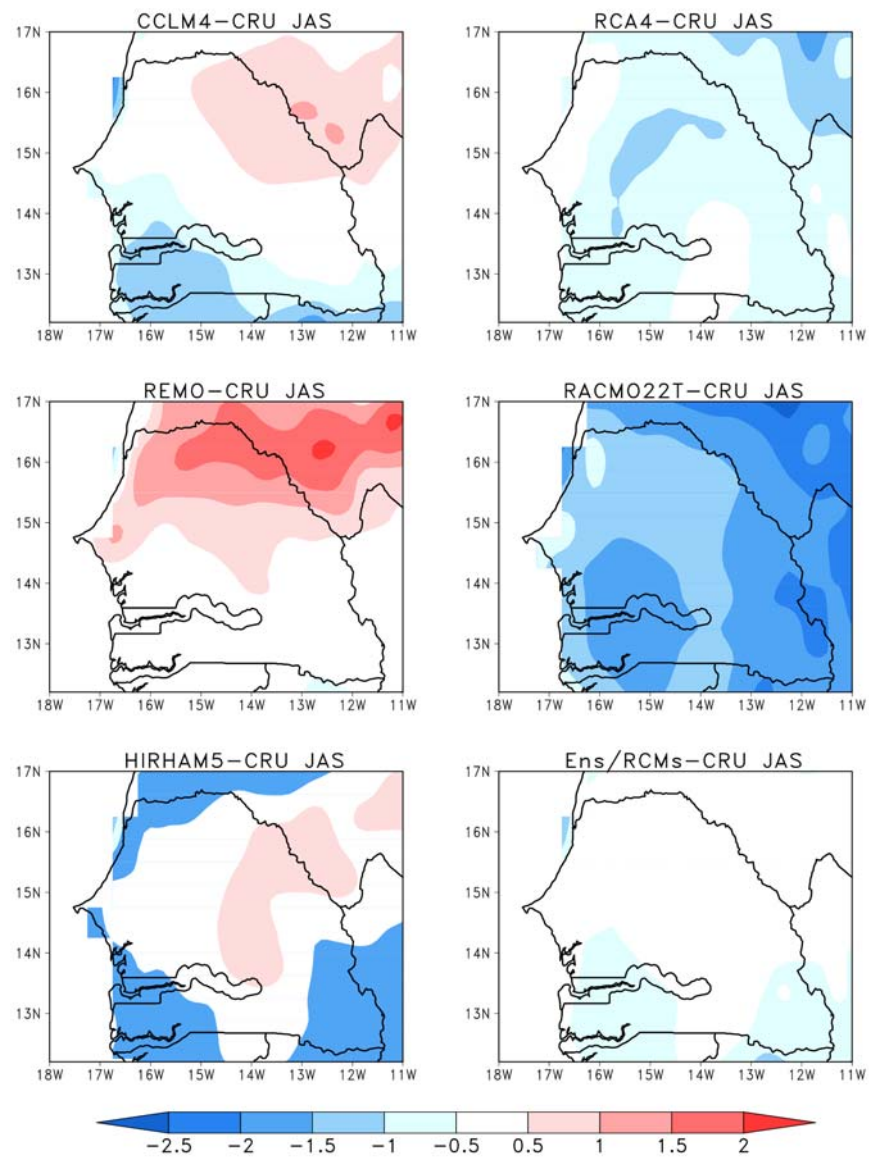


Figure 4. Deviation from CRU observations of mean JAS temperature averaged from 1989 to 2008 of the RCMs and their ensemble mean.

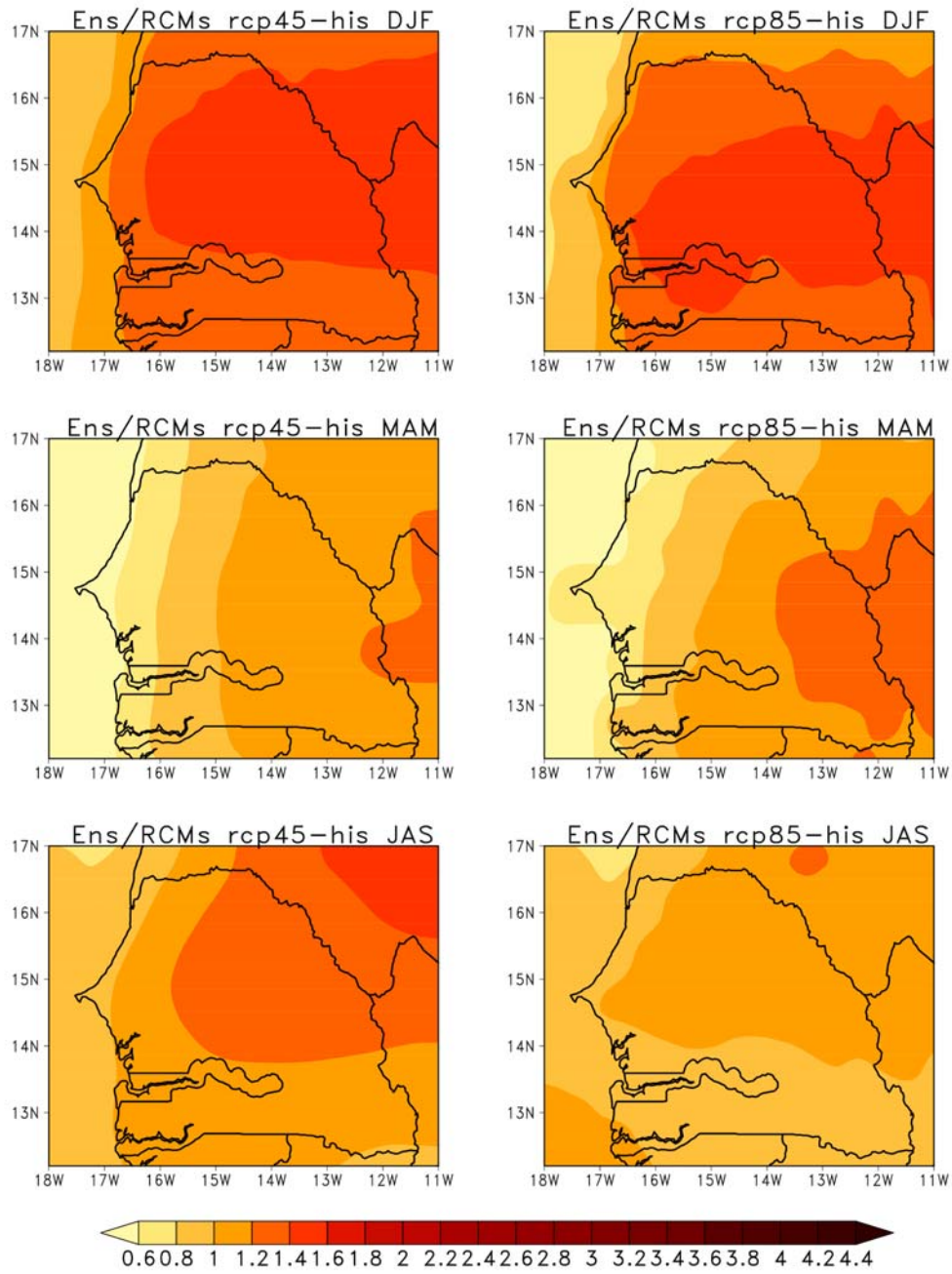


Figure 5. Spatial distribution of the mean surface temperature difference between the near future (2021-2050) and the reference period (1976-2005).

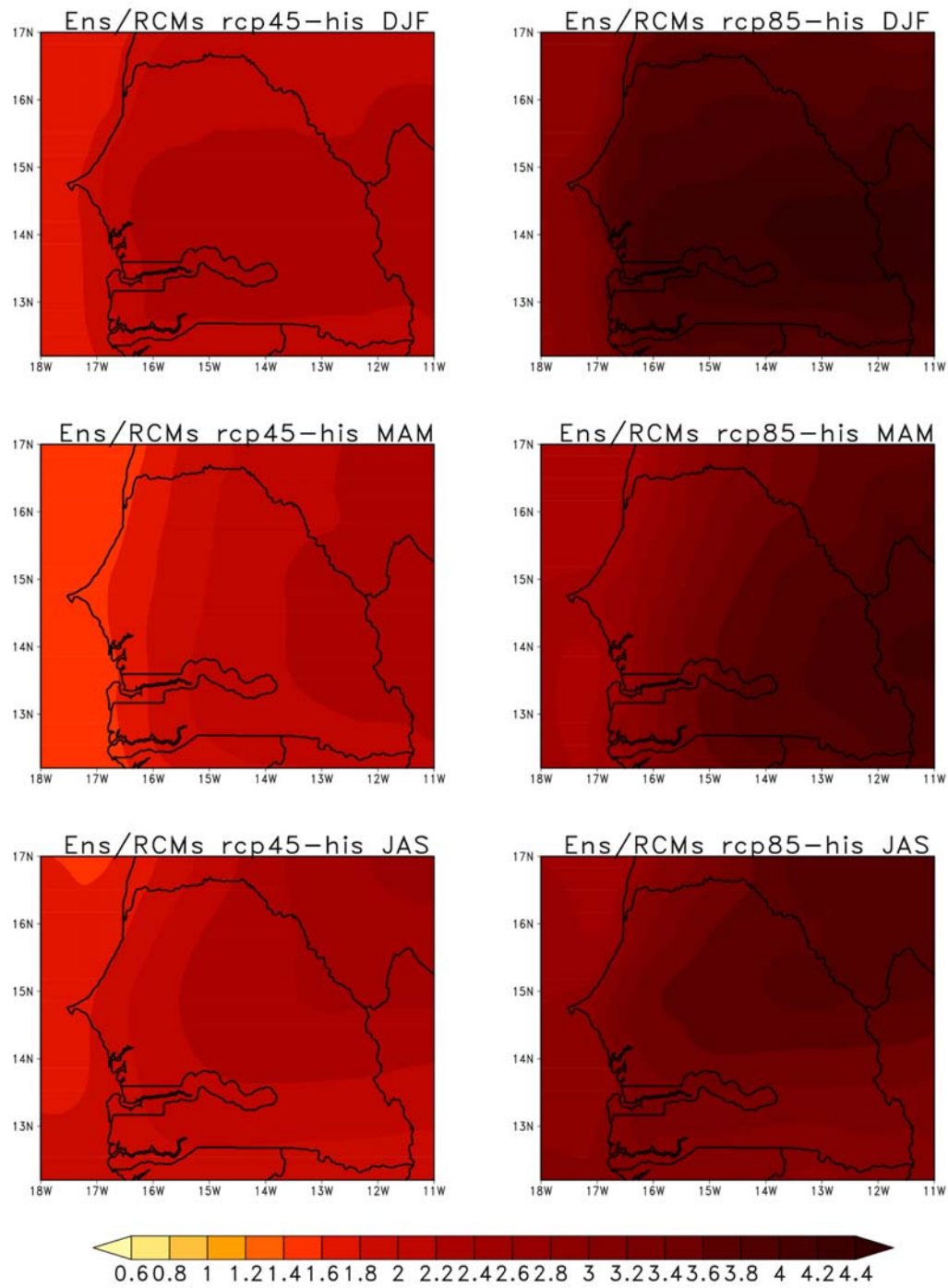


Figure 6. Spatial distribution of the mean surface temperature difference between the far future (2071-2100) and the reference period (1976-2005).

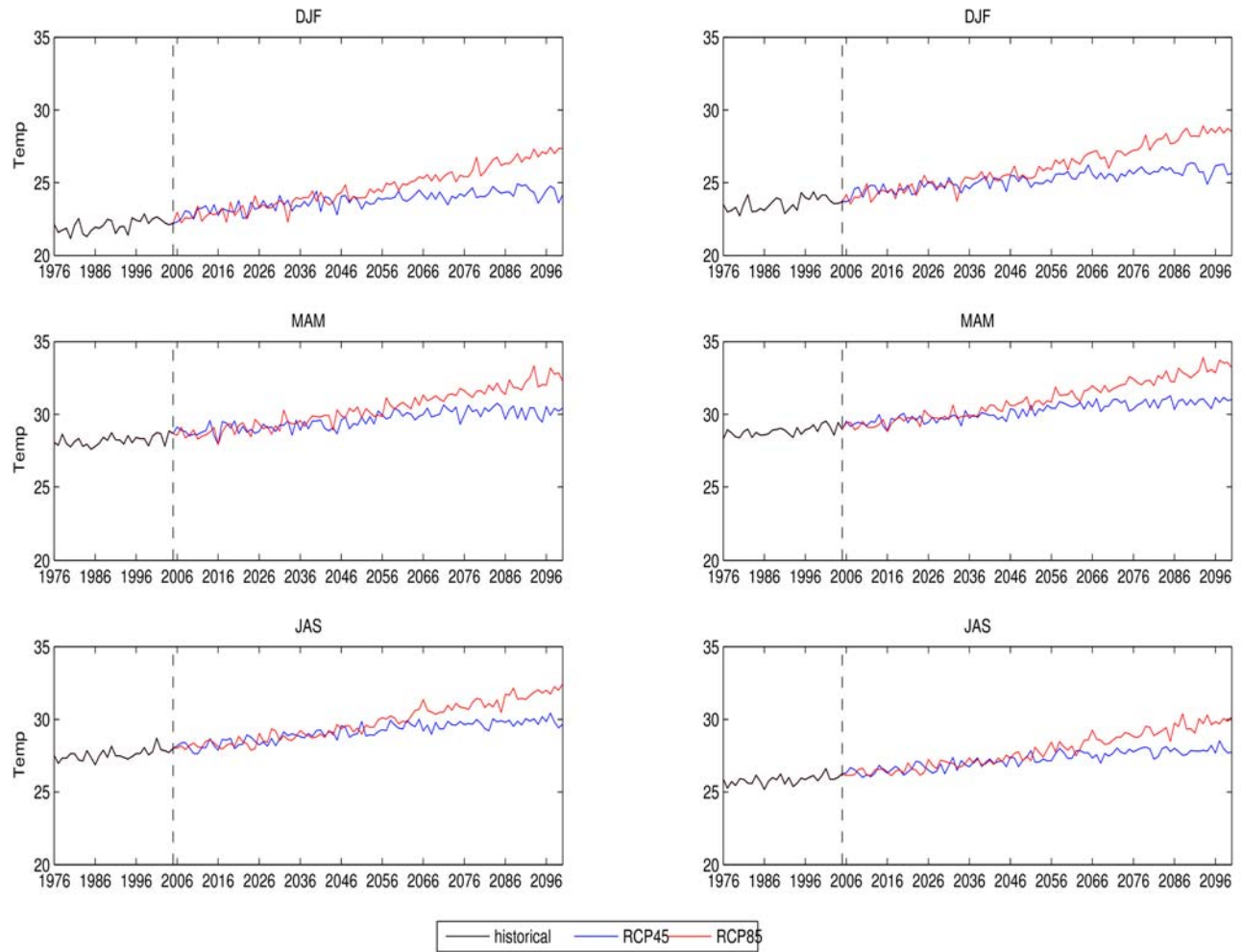


Figure 7. Temporal evolution of the surface temperature ($^{\circ}\text{C}$) during the cold (DJF), hot (MAM) and wet seasons (JAS) in the north (left panel) and in the south (right panel) of Senegal.